DESIGN AND PRODUCTION STAGES OF A VIBRATION TEST FIXTURE

A THESIS SUBMITTED TO
THE GRADUATE SCHOOL OF NATURAL AND APPLIED SCIENCES
OF
MIDDLE EAST TECHNICAL UNIVERSITY

BY

CANER TÜRKER

IN PARTIAL FULFILLMENT OF THE REQUIREMENTS
FOR
THE DEGREE OF MASTER OF SCIENCE
IN
MECHANICAL ENGINEERING

SEPTEMBER 2020

Approval of the thesis:

DESIGN AND PRODUCTION STAGES OF A VIBRATION TEST FIXTURE

submitted by **CANER TÜRKER** in partial fulfillment of the requirements for the degree of **Master of Science in Mechanical Engineering, Middle East Technical University** by,

Prof. Dr. Halil Kalıpçılar
Dean, Graduate School of Natural **and Applied Sciences** ________________

Prof. Dr. M. A. Sahir Arıkan
Head of the Department, **Mechanical Engineering** ________________

Prof. Dr. Ender Ciğeroğlu
Supervisor, **Mechanical Engineering, METU** ________________

Assist. Prof. Dr. Gökhan O. Özgen
Co-Supervisor, **Mechanical Engineering, METU** ________________

Examining Committee Members:

Assoc. Prof. Dr. M. Bülent Özer
Mechanical Engineering, METU ________________

Prof. Dr. Ender Ciğeroğlu
Mechanical Engineering, METU ________________

Assist. Prof. Dr. Gökhan O. Özgen
Mechanical Engineering, METU ________________

Assoc. Prof. Dr. Yiğit Yazıcıoğlu
Mechanical Engineering, METU ________________

Assoc. Prof. Dr. S. Çağlar Başlamışlı
Mechanical Engineering, Hacettepe University ________________

Date: 25.09.2020

I hereby declare that all information in this document has been obtained and presented in accordance with academic rules and ethical conduct. I also declare that, as required by these rules and conduct, I have fully cited and referenced all material and results that are not original to this work.

Name, Last name : Caner Türker

Signature :

ABSTRACT

DESIGN AND PRODUCTION STAGES OF A VIBRATION TEST FIXTURE

Türker, Caner
Master of Science, Mechanical Engineering
Supervisor : Prof. Dr. Ender Ciğeroğlu
Co-Supervisor: Assist. Prof. Dr. Gökhan O. Özgen

September 2020, 91 pages

Random vibration tests are performed by attaching a product on an electro dynamic shaker as a part of standardized environmental vibration tests which require specified random vibration profiles applied to products within certain tolerance bands. An ideal test fixture, which will be used to attach a product to a shaker, should be as rigid as possible with no local resonances in the frequency range of the random vibration test profile. However, such a fixture design is rarely possible due to concerns such as fabrication costs, testing time, etc. A rigid fixture usually leads to a design comprised of massive components which may not be economical to fabricate or may not be feasible because of the available payload carrying capacity of the shaker planned to be used for the test. In cases where multiple test items are sought to be tested simultaneously to reduce overall testing time, increased total payload necessitates the fixture designers to reduce the fixture weight. All these practical issues oftentimes force test engineers to design relatively low-weight test fixtures with local resonant behavior in the frequency range of interest. The existence of these local resonances of the fixture would cause resonant vibration behavior which sometimes may prevent the shaker control system from producing the desired random vibration profile. In this study, a random vibration testing scenario is investigated to identify the described issues with producing a desired random vibration profile. The problem is studied both experimentally and through finite element simulations. A remedy, which involves increasing damping in the problematic local modes of the test fixture by adding tuned vibration absorbers, is proposed and shown to be effective through finite element based simulations and experiments.

Keywords: Random Vibrations, Vibration Test Fixture, Resonance Vibration Problems, Vibration Control, Tuned Vibration Absorbers

ÖZ

BİR TİTREŞİM TEST FİKSTÜRÜNÜN DİZAYN VE ÜRETİM AŞAMALARI

Türker, Caner
Yüksek Lisans, Makina Mühendisliği
Tez Yöneticisi: Prof. Dr. Ender Ciğeroğlu
Ortak Tez Yöneticisi: Öğretim Üyesi Dr. Gökhan O. Özgen

Eylül 2020, 91 sayfa

Standartlaştırılmış çevre koşulları titreşim testlerinden biri olan rastgele titreşim testi, test edilecek birimin elektro dinamik sallayıcıya bağlanıp belirlenmiş rastgele titreşim testi profilinin belli tolerans aralığında birime uygulanmasıyla yapılır. Test edilecek birimin sallayıcıya bağlanabilmesine yarayan test fikstürü idealde olabildiğince rijit olup test frekans bandında bölgesel rezonanslara sahip olmamalıdır. Ancak ideal bir fikstür dizaynı fikstür üretim maliyeti, uzun test süreleri gibi sebeplerden dolayı çok nadir mümkün olmaktadır. Rijit bir fikstür genelde masif parçalardan oluşan bir dizayn gerektirmekte olup bu durum ekonomik olmayan üretim maliyetlerine ya da testte kullanılacak sallayıcının maksimum yük limitinin aşılmasına sebep olabilmektedir. Toplam test süresini azaltmak için birden fazla test edilecek birimin aynı anda test edilmesinin istendiği durumlarda oluşacak yük artışı, fikstür tasarımcılarının test fisktürünü hafifletmesini gerektirmektedir. Pratikte karşılaşılan bütün bu konular, test mühendislerini test frekans bandında bölgesel rezonanslara sahip oldukça hafif test fikstürleri dizayn etmeye zorlamaktadır. Test fikstürünün bölgesel rezonanslarının varlığı bazen test esnasında rezonans davranışlarına sebep olup, sallayıcı kontrol sisteminin istenilen rastgele titreşim test profilini oluşturmasına engel olabilmektedir. Bu çalışmada, belirtilen konuları açığa kavuşturmak için bir rastgele titreşim test senaryosu deneysel ve sonlu elemanlar yöntemi analizleri ile incelenmiştir. Bir çözüm olarak, test fikstürünün problemli lokal modlarındaki sönümleme miktarının ayarlanmış titreşim soğurucuları kullanılarak arttırılmasının rezonans problemini gidermede etkili olacağı simulasyonlar ve testler ile gösterilmiştir.

Anahtar Kelimeler: Rastgele Titreşimler, Titreşim Test Fikstürü, Titreşim Rezonans Problemi, Titreşim Kontrolü, Ayarlanmış Titreşim Soğurucuları

To My Family

ACKNOWLEDGMENTS

The author wishes to express his deepest gratitude to his supervisor Prof. Dr. Ender Ciğeroğlu and co-supervisor Assist. Prof. Dr. Gökhan O. Özgen for their guidance, advice, criticism, encouragements and insight throughout the research.

The author would also like to thank Dr. Güvenç Canbaloğlu and Yusuf Eldoğan, MSc. for their suggestions and comments.

The technical assistance of Aselsan MGEO Environmental Test Lab. and Aselsan MGEO Test Systems and Processes Design Department Mechanical Workshop Personnel are gratefully acknowledged.

TABLE OF CONTENTS

LIST OF TABLES

TABLES

LIST OF FIGURES

FIGURES

LIST OF ABBREVIATIONS

ABBREVIATIONS

FEA: Finite Element Analysis

FE: Finite Element

FFT: Fast Fourier Transform

PSD: Power Spectral Density

SDOF: Single Degree of Freedom

TR: Transmissibility

TVA: Tuned Vibration Absorber

UUT: Unit Under Test

CHAPTER 1

INTRODUCTION

Electro-dynamic shakers, which will be discussed in one of the following sections in detail, are widely used in environmental test laboratories to perform random vibration tests on mechanical systems and products along three test directions (vertical, transverse and longitudinal). In the context of this kind of shaker testing, the mechanical system or the product being tested can be defined also as the Unit under Test or UUT in short. Test directions are mutually orthogonal and they are defined either by the designing party or relevant standards the UUT has to abide. Test profiles for each test direction are obtained by either direct measurement in operational conditions of the UUT or applicable test profiles can be selected from the respective test standards. An electro-dynamic shaker has a single axis of motion and proper orientation of the shaker and connection of the UUT to the shaker should be arranged to conduct tests in the required three test directions. Typically, shaker body can be rotated as 90 degrees for switching between vertical and horizontal (transverse and longitudinal) test axes as it can be seen in Figure 1.1. Switching between horizontal test axes can be obtained by rotating the UUT mounted on the slip table plate which is connected to the horizontally oriented shaker. Shakers and accompanying accessories for performing vibration tests on UUTs in different direction are discussed in the next chapters.

In order to connect shaker table (armature in vertical testing, slip table plate in horizontal testing) and the UUT, a connection fixture is needed which has two interfaces, one for the shaker table and one for the UUT. This connection fixture, which can be seen as the transparent body in the Figure 1.1, is times called the “vibration test fixture” in practical applications. Ideally, a vibration test fixture should have no resonant frequency within the frequency range of the test being condcuted. One may say that, a vibration test fixture should be as rigid and lightweight as possible so as not to modify vibration levels the UUT is being exposed to due to local resonant response of the vibration test fixture. However, reasons which are listed below generally lead less than ideal conditions, i.e. to flexible vibration test fixtures with unavoidable resonance characteristics being observed in the frequency range of the test being conducted:

- Shape constraints
- Mechanical property limits of the fixture material
- High inertial loads of the test item
- Mass limitation of the vibration test fixture caused by the shaker dynamic load producing capacity (force) and and load requirements implicated by the target vibration test profile (acceleration)
- Improper joining methods of the fixture parts causing unwanted compliance in the vibration test fixture

If the resonant behavior and response stemming from the dyamic characteristics of the vibration test fixture is severe, shaker controller may not be able to produce desired vibration test profile, which is basically done by adjusting the drive voltage signal. Such a scenario results in vibration test not being successfully performed.

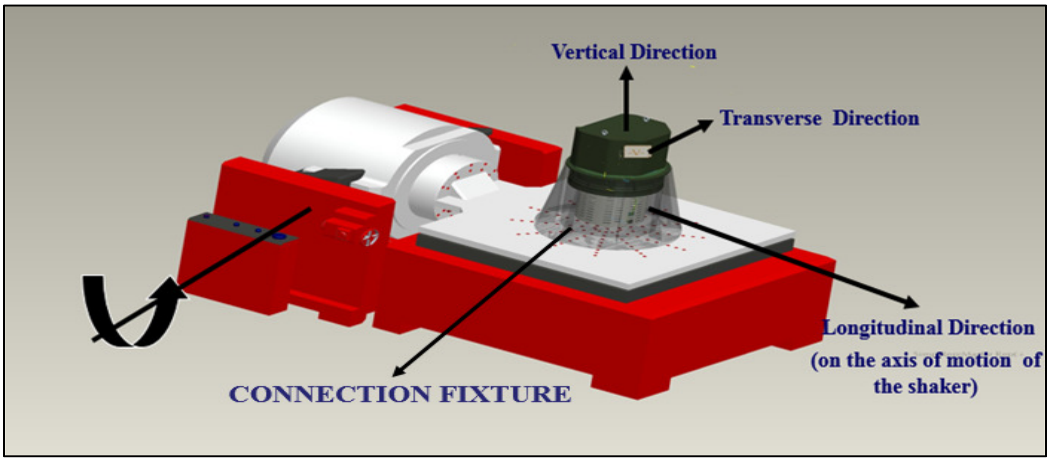

Figure 1.1. A commercial electro-dynamic shaker with vibration test fixture and UUT

The main ojective of this thesis study is to reduce this problematic severe resonant behavior caused by vibration test fixtures. Doing so is expected to avoid situations where vibration tests are aborted because desired vibration test profiles can not be applied to the UUT. To develop a method for reducing resonant vibration repsonses of vibration test fixtures, a problematic test setup (electro-dynamic shaker+vibration test fixture+UUT assembly) is analyzed and studied, which has severe multiple resonant responses within the test frequency range preventing the shaker control system producing the target radom vibration test profile on the UUT. In the initial scenario, due to the existence of the severe resonant behavior in UUT, shaker, vibration fixture assembly, the shaker controller can not obtain the desired test profile and the test is aborted. Desired random vibration test is tried to be obtained (avoiding aborted test attempts) by suppressing resonant behavior of the problematic resonant modes of the UUT, vibration test fixture and shaker assembly.

Before analyzing the problem and suggesting a solution method, a comprehensive literature review is completed in the field of vibration test and vibration test fixture design with focus on similar situations where resonant vibration characteristics of vibration test fixtures are of concern. Relevant studies are reported and summarized in Chapter 2.

To help develop the method using the UUT case study, dynamic modeling and characteristics of electro-dynamic shakers used in similar test situations must be taken into consideration. For this reason, Chapter 3 is devoted to modeling and analysis of dynamics of electro-dynamic shakers. Firstly, electro-magnetic force theory is presented which is the theory behind the electro-dynamic shakers to generate force for motion. This is followed by discussion of typical commercial electro-dynamic shakers and auxiliary test equipment. Dynamic modeling of electro-dynamic shakers is then discussed and a electro-mechanical model is presented. In addition, conceptual design details of the inner structure of the shaker is presented. Lastly, electro-mechanical equations, force & current, voltage & velocity relations are presented.

In Chapter 4, random vibration tests are explained which are most commonly required vibration tests for UUT. This chaper starts with the statistical modeling and characteristics of random vibration signals and continues with the modeling and definition of the typical random vibration test profiles used in UUT shaker tests. Control algorithm and different control strategies used in shaker control systems for generating random vibration profiles on UUTs are explained.

Detailed explanation of the problematic UUT random test scenario is presented in Chapter 5. Design criterias and limitations of the vibration test fixture are discussed and presented. The FE model of the electro-dynamic shaker used in this test scenario is derived first in this chapter and later FE model of the whole test setup (UUT, vibration test fixture and shaker) is validated through experiments. After validation of the model, increasing damping in problematic vibration modes observed in tranmissibility measurements of the UUT-vibrations test fixture assembly is presented as a remedy (where these modal frequencies are also the frequencies around which deviations of the the applied random vibration profile from the target vibration profile are observed). To introduce damping to the target modes of the UUT-vibration test fixture-shaker assembly, single degree of freedom tuned vibration absorbers (TVA) are used. In simulation-based trials, TVAs are tuned to problematic frequencies and inserted into the validated FE model of the UUT-vibration test fixture-shaker assembly. These trials are performed through FE simulations till the desired dynamic behavior (reduction in problematic resonant peaks in transmissibilty functions) is obtained. Then, the TVAs are fabricated to have the identified effective properties and applied on the actual test setup. Experiments are performed to check the effect of the increased damping and to see the aborted tests are avoided when the designed TVAs connected test setup is used in the random test conducted. In addition, effectiveness of various TVA combinations (TVAs tuned to different resonant frequencies) are analyzed through both FE simulations and the experimentally trials.

In Chapter 6, conclusion and discussion parts are presented in the light of outcomes of this study.

CHAPTER 2

LITERATURE REVIEW

In literature, there are various studies which were made in the field of vibration tests and vibration test fixture design. A brief summary of the studies can be found in the following paragraphs. It is realized that the method developed (increasing effective damping of resonances of the problematic modes of UUT-vibration test fixture-shaker assembly using properly tuned TVAs) has not been used for solving vibration test fixture resonance problems.

Sisemore & Harvie (2017) stated about a problem that arises during multiple components vibration testing. In industry, it is a common way to test smaller items, two or more together in order to save cost and time. However, mode shapes and natural frequencies of the each test item vary slightly due to manufacturing differences and these closely spaced vibration modes interfere each other which may result one of the test item to be over-tested or under-tested. In a vibration test, both under-test and over-test situations imply that desired test conditions are not met and an unsatisfactory vibration test was performed.

Jingze et al. (2016) reported a study about random vibration test fixture design for an airborne heat exchanger. They made some inferences about the design criteria of vibration test fixtures. In one of the criterion, it is concluded that the first resonant frequency of the vibration test fixture shall be higher more than three times than the first order resonant frequency of the test item in order to minimize coupling effects and prevent under-tests or over-test within the test frequency range. However, there may be resonant frequencies of the vibration test fixture within the test frequency range which may result undesired test levels. Moreover, dynamics effects of the test item which modify mass and stifness matrices of the full test system were not taken into consideration during FEA analysis of the vibration test fixture. Lack of test item effects results poor analysis during the vibration test fixture design phase. In addition, the best material distribution for given constraints to reach maximum rigidity was not taken into consideration which can be obtained by topology optimization methods and further tuning of the vibration test fixture by parametric optmization techniques were not used in the study.

Rahman & Kumar (2016) completed a study about composite vibration test fixture design for a combat vehicle fuel tank. Instead of most common metallic alloys based on aluminum and magnesium, glass & carbon fibre with epoxy resin was selected as the vibration test fixture material. They performed several trial and error iterations to shift first resonant frequency of the fixture beyond 2000 Hz without dealing with the topology and parametric optimization techniques. Dynamic effects of the test item were not also taken into consideration in this study too, and mass of the finalized vibration test fixture is only 1.5 times greater than mass of the test item which can change the mode shapes and lower the natural frequencies of the full test system, thus undesired vibration level can be arisen during tests. On the other hand, composite material which was used is not isotropic. Therefore, orientation of the layers are very crucial during design and manufacturing processes. Furthermore, drilling of shaker and test item connection holes cannot be done easily by traditional machining process, special processes such as laser drilling must be performed for composite materials in order to prevent delamination.

A study on optimal design of a head expander was published by H. S. Jeong & Cho, (2016). In the study, size and shape optimization of the head expander was carried out to have a lightweight structure with improved resonant frequency objectives. Three head expander models were defined initially and design parameters were defined next to investigate the change of objectives with respect to design parameters. Then, quadratic regression polynomial was created to reach objectives instead of using FE modal analysis. However, there might be a better model shape other than previously defined three models, and shape of this model can be found out by topology optimization and the model can be tuned by parametric optimization techniques. The analysis must also be performed by considering the dynamic effects of a dummy test item to simulate the real conditions during the tests.

Harvie & Mayes (2016) state that vibration tests cannot be performed at desired levels due to mechanical impedance difference of the test item interface on the fixture & shaker assembly and the test item interface on real environment assembly. This difference is as a result of modes of the shaker & fixture system which cannot be eliminated by shaker control methods. By using substructuring techniques, boundary condition impedance are investigated. Later, some case studies were performed to match the response of the test item in real environment and the response of the test item on test system by changing input level and input locations of the test system. However, this method seems to be only theoretical because there is one controlled input at the boundary of the test system in shaker based vibration tests for an axis. The number of input cannot be increased, but it can be tuned approximately to reach desired vibration levels by using shaker control methods.

Structural dynamic modification of a vibration test fixture was performed experimentally by Kim et al. (2001). As it is said in the previous paragraphs, vibration level at the test item mounting points changes due to the presence of vibration test fixture resonances/modes within the test frequency range. Under-test levels are seen especially at anti-resonance frequency during tests. In order to overcome this problem, structural dynamic modification was implemented by using transfer function synthesis method. Response level at desired point on the fixture was predicted by using experimental data and the transfer function synthesis method. In order to meet the objective function and obtain desired spectra at the test item mounting points, masses in different sizes are added rigidly to the vibration test fixture at previously defined points. This study only focused on under-test at anti-resonance frequencies, but there can be severe resonant behaviour which must also be handled as a problem. In addition, test item dynamic effects must also be taken into consideration for reliable analysis.

W. B. Jeong et al. (2003) published a study about sensitivity analysis of anti-resonance frequency for vibration test control of a vibration test fixture. They stated that response spectra of the test item attachment points on the fixture must be all the same, then desired vibration spectra can be obtained by altering single input of the shaker. In contrast there are resonant and anti-resonant frequencies of the fixture within the test range which result over-test and under test respectively. It is stated that anti-resonant behavior is more important because transmissibility can be very large or infinite which is far beyond to be controlled by single shaker signal whereas transmissibility at resonant frequencies is not infinite and can be possibly controlled by single shaker signal. An aluminum plate, which has 4 test item mounting points and divided into sub elements, was taken as the vibration test fixture. Firstly, length and width of the vibration test fixture were modified and then thickness of the triangular elements were modified to have the same response at the mounting points. Indeed thickness modification of sub elements is not practical due to triangular shape of the elements. Sharp corners are hard to obtain for cutting operations and 0.01 mm precision may not be met for larger plates. In addition, dynamic effects of the test item were not considered as an open side of the study.

De Barros & Souto (2017) published a study about evaluation of vibration test fixtures. He mainly discussed transmissibility of the different points with respect to reference signal and implied that transmissibility at resonant frequencies are different for points located differently and unsymmetrically. Thus, response at resonance frequencies can be different for mounting points which were discussed previously. It can also be said that dynamic effects of the test item must be considered throughout the study.

Williams et al. (2019) implemented a control algorithm for their old fashioned vibration controller to have multi-point control ability which is readily available in commercial shaker controllers.

Kulkarni & Lakkannavar (2015) made a study to obtain desired dynamic response of a vibration fixture by topology optimization and fine tuning of the model. A model was created with respect to topology optimization results and also frequency response analyses (transmissibility) of the test item mounting points were performed to check response at resonant and anti-resonant frequencies are within the test limit. Throughout the study, dynamic effects of the test item were not considered which can change the results apparently.

DeLima & Ambrose (2015) were used modal analysis and operational deflection shape analysis in order to model a full test system including shaker, shaker adapter plate and vibration test fixture. This model is used to simulate the real test of a test item which is faster than preparing a full test setup in real life. This study also states cross axis vibration level during a vibration test experimentally, which must be taken into consideration during multi-axial vibration test. On the other hand, there is no part in this study about vibration test fixture design or overcoming resonant/anti-resonant problems in vibration tests.

Avitabile (1999) examined the presence of vibration test fixture resonances within the test range and coupling effects with the test item modes. He stated that “ a perfect fixture has no mass and infinite stiffness” which means that the vibration test fixture should be as rigid as possible and first resonant frequency of the fixture must be beyond the test range as much as possible. He also clarified that a control accelerometer can only control the point where it is attached. The resonant behaviour of the fixture stays still in the system. Moreover, he mentioned that it is sometimes impossible to have a resonant free fixture due to physical limitation, structural modification may be needed or mounting the test item may increase the rigidity. He also showed that a more rigid fixture, which has a higher first resonant frequency, has a slight effect because of coupling with the test item modes as it is compared with a more flexible fixture with lower first resonant frequency.

Poncelet et al. (2005) performed a topology optimization based vibration test fixture design. After reaching design objectives satisfactorily, the vibration test fixture was manufactured and verified experimentally.

In their study, Wang et al. (2013) performed topology optimization to have the initial layout of the vibration test fixture according to objectives and constraints. After topology ptimization, they model the vibration test fixture parametrically and performed a parametric optimization to tuned objectives finely. They also stated that this design methodology can be used for dynamic design of other structures as well.

In order to prevent over-testing around resonant frequency of the fixture, Zhang & Ma (2012) studied on forced limited vibration testing. During the test, force level is decreased around the fixture resonance. This method might be useful if there is a single mounting point for the test item. However, there are usually more than one mounting points of the test item which have different transfer functions and different amplification levels around the resonance. Limiting the force according to one mounting is a way to obtain desired vibration test profile at that point, but vibration test profiles at other mounting points may not match the desired level.

Due to the fact that different transfer functions of the test item mounting points are the result of vibration test fixture resonances presence, Li et al. (2013) developed a method about where the control accelerometer must be mounted to satisfy the conditions that all mounting points of the test item have desired vibration test levels. This method can be used for mild vibration fixture resonance behaviour within the system, in the case of a severe vibration fixture resonance problem there may be no location for the control accelerometer to meet the vibration test level requirements.

Yuan & Li (2003) examined the vibration test levels at test item attachment points. Due to dynamic behaviour of the vibration test fixture, it is concluded that vibration test levels at test item attachment points differ from reference vibration test profile. A method, which modifies the reference vibration test profile in order to minimize the deviation at test item mounting points, was presented in this study. Results of the study shows that a limited improvement can be achieved by using this technique and vibration test levels at test item mounting points are not still in the test tolerance limits which are defined by military standards. Proposed method seemed to work good for the locations where over-tests occur, but for under-test regions around anti-resonance frequencies this method was not able to modify the signal to obtain desired test levels. In addition, similar techniques with similar performances such as multi-point control etc. have been embedded into today's commercial vibration controllers.

In their studies, Kumar et al. (2002) and Gatscher & Kawiecki (1996) stated that vibration test profiles which are taken from standards are the envelope of real measurements. Thus, over-tests are performed automatically without noticing. Some methods were proposed in both studies which use real life measurements to create vibration test profiles with minimized over-test effects.

Consequently, due to severe resonant behavior of the test setup including shaker, vibration test fixture and UUT, the problem of producing undesired random vibration test profiles has not been handled yet. This study deals with the stated problem and it consists of a novel approach for vibration test industry.

CHAPTER 3

ELECTRO-DYNAMIC SHAKERS

Electro-dynamic shakers are widely used in industry for performing environmental vibration and shock tests. There are shakers with high load capacity in order to perform vibration tests of massive test items such as a satellite system and investment cost of the shakers are increasing by the load capacity. In addition, more complex multi-shaker systems are also available for special purposes. Shakers can also be used for modal testing purpose. Due to the fact that the force generated by an electro-dynamic shaker during a test can not be measured, modal shakers are used with a force transducer mounted on top of the shaker stinger where the shakers excite the test item.

In the following sections; electro-magnetic force theory, a commercial electro-dynamic shaker and dynamic modeling of electro-dynamic shakers will be explained. All the given information is useful for test engineers in order to know what is behind the scene of electro-dynamic shakers. In addition, the general dynamic model given in this chapter will be simplified with a reasonable approach in order build FE model of the electro-dynamic shaker.

3.1 A Brief Theory of Electro-magnetic Force

As a traditional example, operation of an electro-dynamic shaker is similar to operation of a loud speaker. When an electric current passes through a wire or coils (many turns of wires), a magnetic field is created which is opposed to static magnetic field that is created by the field coil in the shaker and the force which moves the coil is generated. The moving coil and armature move together where we mount vibration test fixture and test items. In Figure 3.1. basic structure of an electro-dynamic shaker can be seen.

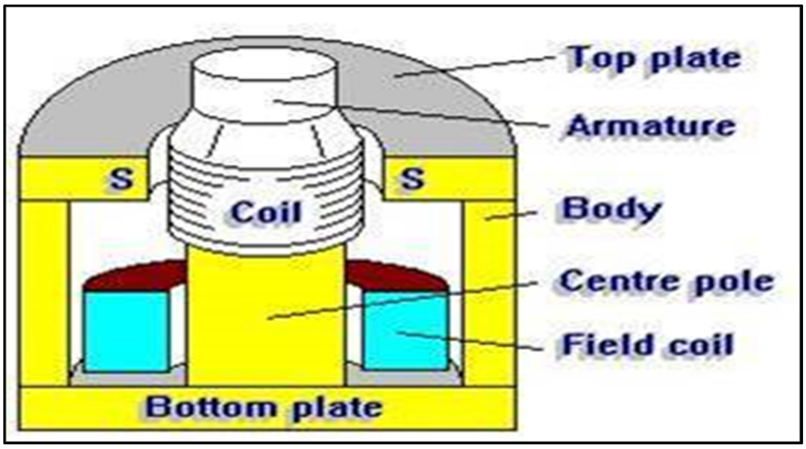

Figure 3.1. Schematic of a basic electro-dynamic shaker (Baker, n.d.)

The force created in the coil to move armature is proportional to passing current, magnetic field and the coil length. Related formula for the generated force will be introduced in the next section. However it is better to introduce force, magnetic field and current directions here which are according to Fleming's Left Hand Rule as in Figure 3.2.

Figure 3.2. Fleming's left hand rule (Baker, n.d.)

Fleming's Left Hand Rule for the electro-dynamic shaker can be visualized in Figure 3.3.

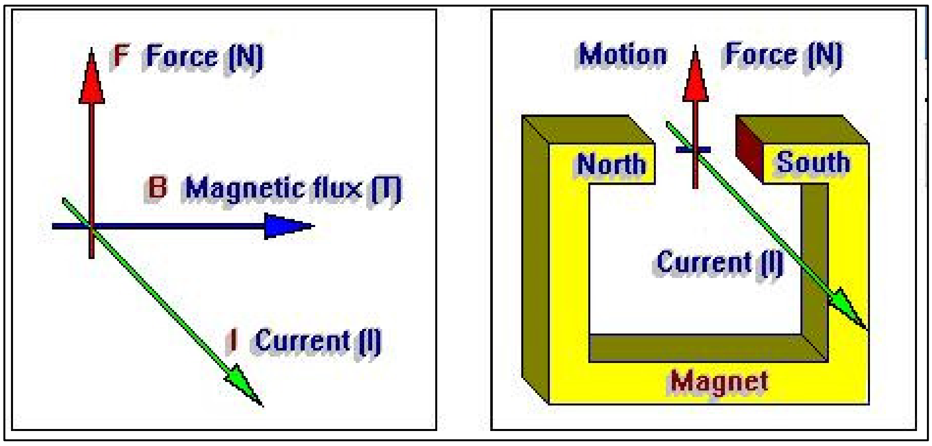

Figure 3.3. Direction of force, magnetic field and current (Baker, n.d.)

3.2 Commercial Electro-dynamic Shakers

Designing and validating of a shaker are not quite simple processes, these processes both require intense knowledge in structural dynamics, control theory, electrical power engineering and cooling. Hence, there are only a few shaker manufacturers which lead the shaker based vibration tests in the industry.

A shaker basically consists of three main parts which are a shaker base, a power amplifier and a control system. Electro-magnetic force which is required for tests is generated within the armature inside shaker base as it was mentioned in the theory section. Direction of the generated force hence the direction of motion is along the gravity. The power amplifier consists of power modules, the gain (amplification ratio between input voltage to output voltage) should be maximized to use the full force capacity of the shaker. Cooling can be achieved by air cooling which requires a fan system. Water cooling is used for high load capacity shakers. Control system of the shaker simply controls the dynamic behavior of the shaker for proper tests. It contains a control module, one directional control accelerometer(s) and a PC for changing test parameters by the use of a commercial software set. A commercial electro-dynamic shaker can be seen in Figure 3.4.

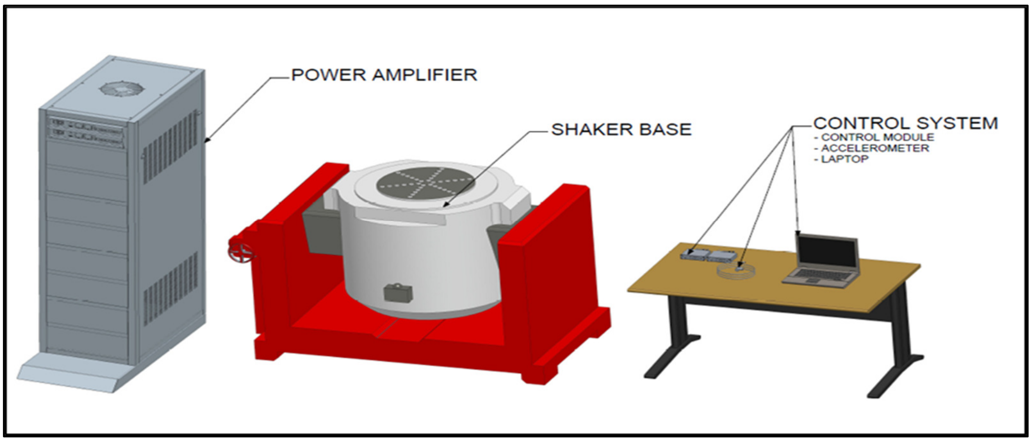

Figure 3.4. A commercial electro-dynamic shaker

In addition to those three main parts, there are some extra parts which can make the vibration tests more applicable. One of them is the adapter plates, they are mounted on the armature base as in Figure 3.5 and they are used to have proper mounting surface for vibration test fixture installation.

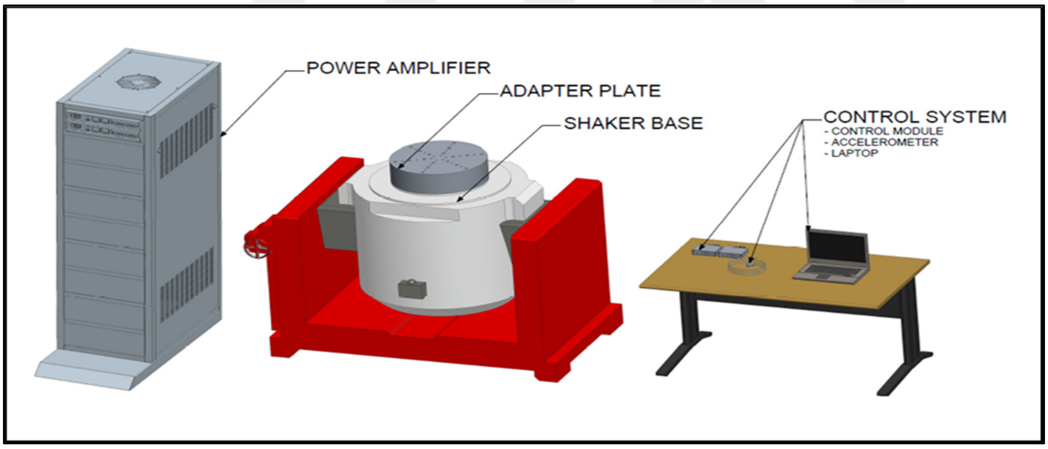

Figure 3.5. A commercial electro-dynamic shaker with an adapter plate

Head expanders are also used for the same for purpose but for testing of larger vibration test fixture and test item combinations. A head expander mounted shaker system can be seen in Figure 3.6. All these extra parts are designed for vertical direction tests. There is an important precaution for test in vertical direction. Turning moments, which are created during tests due to off-axis center of gravity of the total moving mass, must not exceed the shaker's turning moment limits in order not to damage the armature. These types of damages may result high repair cost, nearly the price of a new armature. Expander heads with linear guides are used to prevent potential damages of the shaker by the help of linear bearings which support the turning moments during tests.

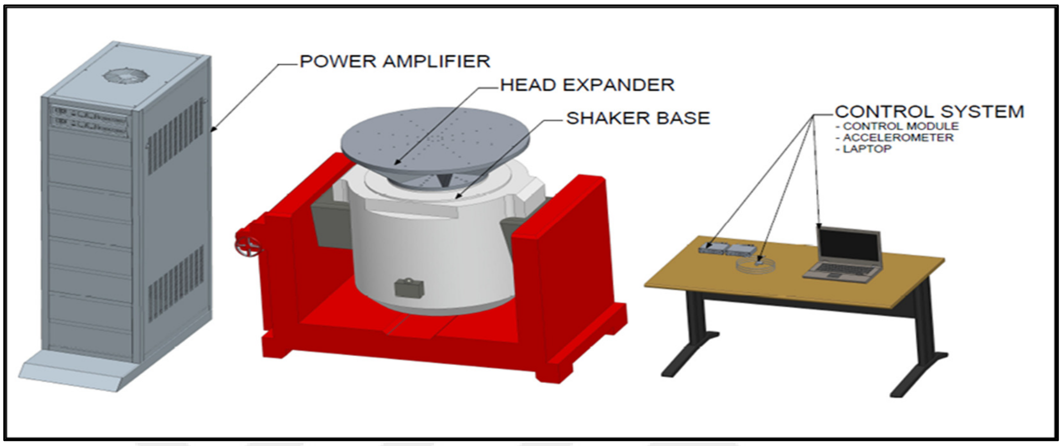

Figure 3.6. A commercial electro-dynamic shaker with a head expander

Moreover, using horizontal slip tables is also another solution for preventing armature damage. In this case, the shaker base is rotated 90 degrees and connected to a slip table which has linear guides for rigidity and oil film between the moving slip table plate and slip table base to minimize friction during tests. A slip table mounted shaker system can be seen in Figure 3.7.

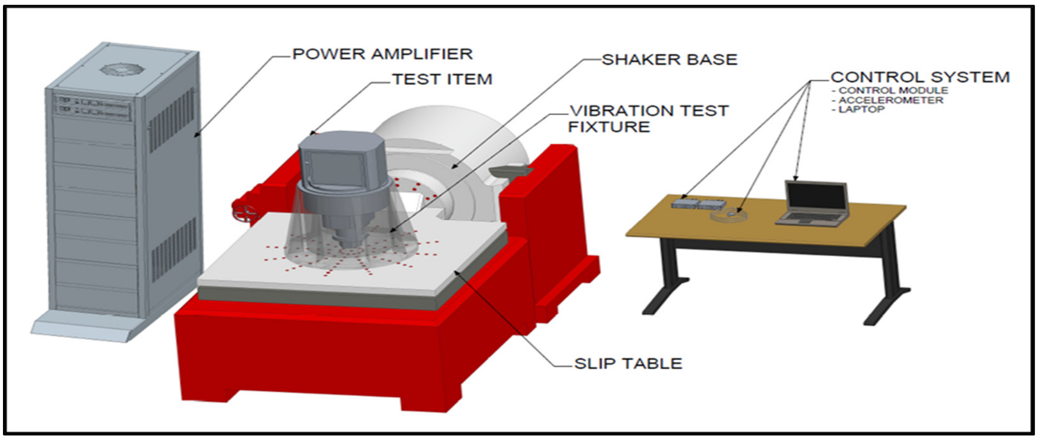

Figure 3.7. A commercial electro-dynamic shaker with a slip table

3.3 Dynamic Modeling of Electro-dynamic Shakers

In this section major parts of an electro-dynamic shaker are introduced. Followingly, related mechanical and electrical models are considered. Modes and mode shapes of the shaker and essential force & current, voltage & velocity relations are presented.

3.3.1 Shaker Components and Electro-mechanical Model

Components of a generic shaker can be seen in Figure 3.8. The armature is the moving part of the shaker. It has an upper table for mounting vibration fixture and test item and a coil structure for generating force. The armature is supported by an air spring for internal load supporting purpose. Different loads can be supported and centered with respect to vertical stroke of the shaker. Upper and lower suspensions are guides and bearings which are used to align the armature concentrically with respect to shaker body. Stiffness of the armature is increased for high rigidity along rotational axes and lateral translational axes by suspension systems. Only constraint of the armature for vertical movement is low air spring stiffness. Thus, the armature is considered to move freely in vertical direction. Bunds of copper wire are called as voice coil and they are located at the bottom side of the armature. The voice coil is exposed to static magnetic flux which is created by field coils. An axial force is generated if a current passes through voice coils as it is explained in section 3.1.

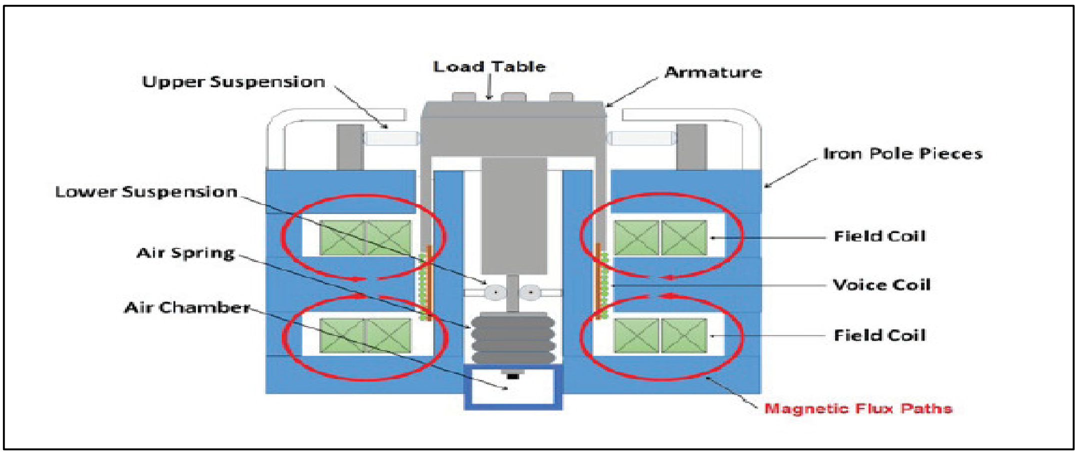

Figure 3.8. Schematic of an electro-dynamic shaker (Sentek, n.d.)

Voice and field coils are both driven by the shaker amplifier. DC current is supplied for the field coils and AC current is supplied for the voice coil, which is regulated according to the controller drive voltage.

Dynamic modeling of a shaker consists of both mechanical and electrical coupled systems as in Figure 3.9. Driving force of the mechanical system is generated by the current in electrical system. In addition, the back emf excites the electrical system and it is proportional to voice coil relative velocity with respect to shaker body. For the lumped mass model of the shaker, M_B stands for shaker body mass. K_B and C_B are stiffness and damping of the ground isolator respectively. K_S and C_S stand for stiffness and damping value of the armature air spring support respectively. The armature is modeled as two masses M_T (table mass, where the vibration test fixture and test item are mounted) and M_C (coil mass) which are connected by the spring element K_C and damping element C_C which represent the table and voice coil connection structure. For the electrical model, R is the resistance and L is the inductance of the voice coil. Two constans, k_1 and k_2 are force & current and voltage & velocity constants respectively and they will be mentioned in the following section.

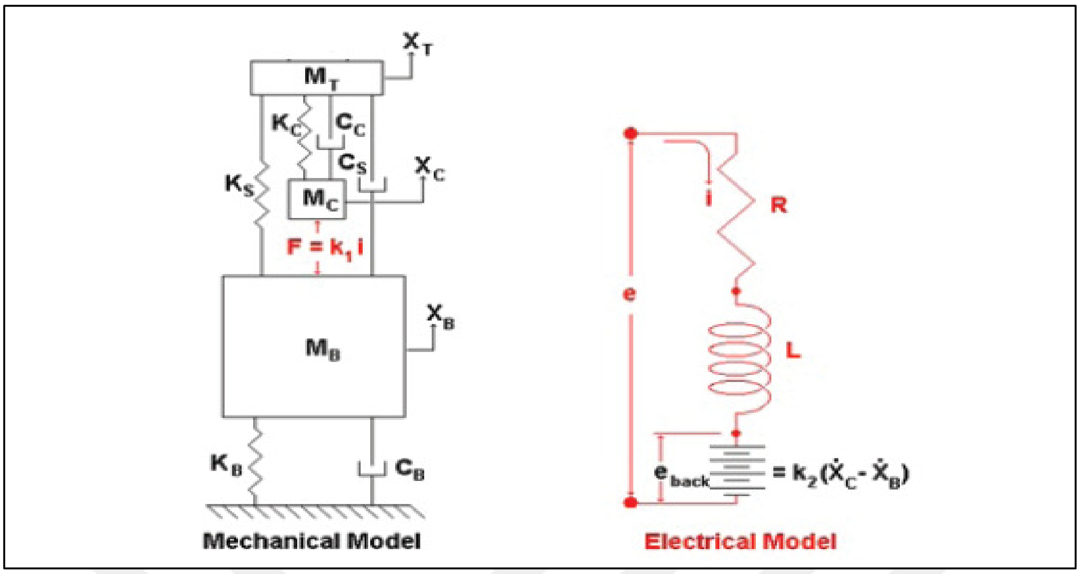

Figure 3.9. Electro-mechanical model of a shaker (Sentek, n.d.)

Dynamic response of a shaker is dominated by 3 mechanical modes which are reflected in electrical model too. These three modes can be named from low to higher modes as: isolation mode, suspension mode and armature mode. (Sentek, n.d.)

Around 3-5 Hz, shaker moves as a rigid body because of soft isolation supports. Figure 3.10 is a representation of the isolation mode.

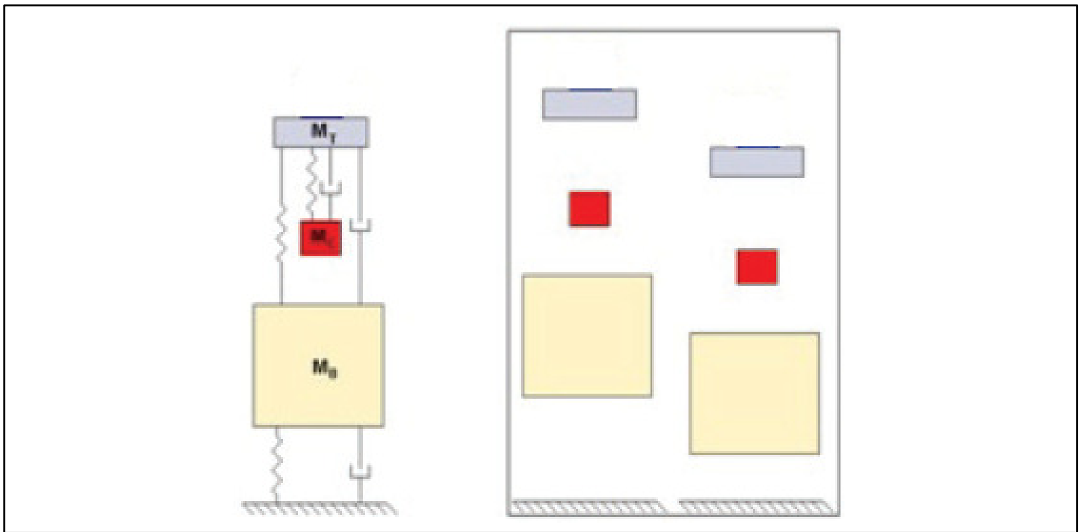

Figure 3.10. Isolation mode shape of the shaker (Sentek, n.d.)

The suspension mode occurs near the lower end of the shaker frequency range because of the air suspension which support the armature. During this mode table and voice coil move together as a rigid body with respect to shaker body. Physical stroke limit of the shaker defines the maximum translation at this mode. As a remarkable point, when the payload is mounted on the table and the stroke of the shaker is centered by manually or automatically, suspension mode frequency is kept nearly the same. It is because of the fact that, when the mass is increased, the stiffness of the air suspension is also increased in proportional to the mass increase to center the stroke of the shaker. The suspension mode can be seen in Figure 3.11.

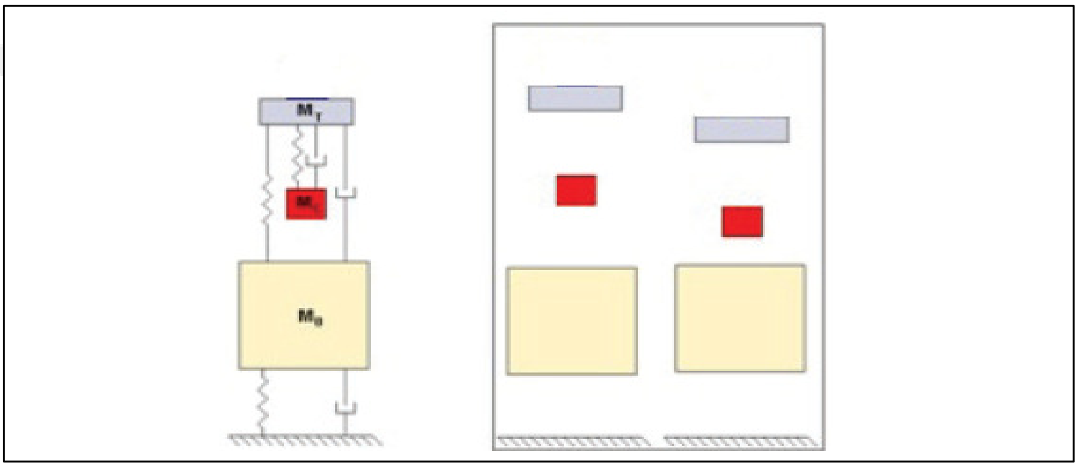

Figure 3.11. Suspension mode shape of the shaker (Sentek, n.d.)

Around upper limit of the shaker frequency range, there is an unwanted mode of the shaker which is the most critical mode in many cases. This mode is called as armature resonance and it is due to internal dynamic characteristics of the armature. At this mode, voice coil and table move out of phase which can damage the armature structure if high excitation exists. A representation of the armature mode can be seen in Figure 3.12.

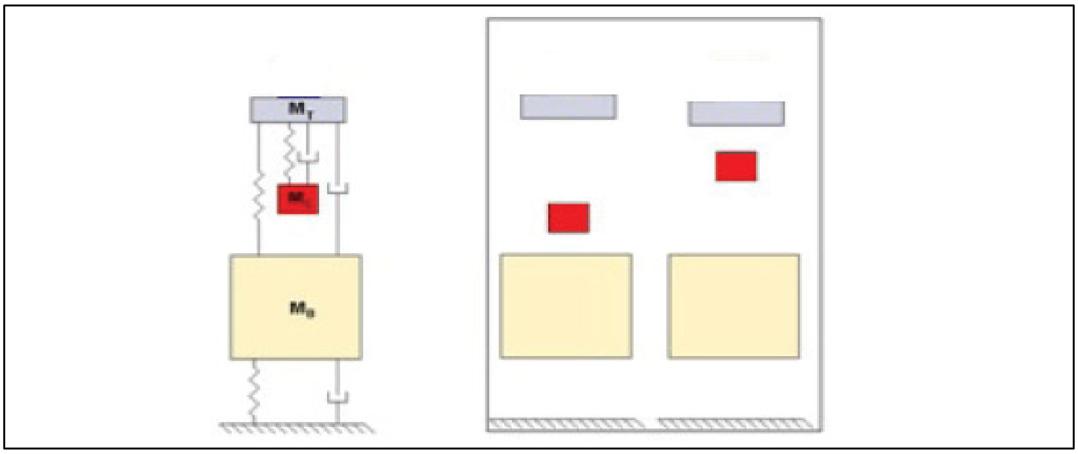

Figure 3.12. Armature mode shape of the shaker (Sentek, n.d.)

3.3.2 Force & Current, Voltage & Velocity Relations

According to Ampere and Lenz laws, mechanical force & velocity and electrical current & voltage interact at the voice coil – magnetic field interface.

Ampere law states the relation between force generated at voice coils and the current passing through voice coils in the existence of magnetic field, B . Generated force can be calculated by using Equation (3.1) (Kenneth G. McConnell, 2008).

$$F = (B.l.n).I = k_1.I \tag{3.1}$$

In Equation (3.1), F is the generated force in Newton, n is the number of coil turns, l is the length of the coil in meter, B is the magnetic field strength in Tesla and k_1 is the force & current constant.

Magnetic field strength, B and flux linkage, Ψ are related through the magnetic theory. In addition, magnetic field strength, B changes with the coil position as in Equation (3.2) (Kenneth G. McConnell, 2008).

$$B = \frac{d\Psi}{dx} = \left[1 - \left\{\frac{x + x_0}{x_{max}}\right\}^2\right] B_0 \tag{3.2}$$

It can be seen from Equation (3.2) that magnetic field strength is nonlinear with the voice coil position, x. (Kenneth G. McConnell, 2008) In Equation (3.2), B_0 is the largest magnetic field strength, x_0 is the offset position with respect to center position of shaker stroke, x is the actual displacement of table and $x_{\max}$ is the maximum achievable table motion.

By combining Equation (3.1) and (3.2), it is seen that force & current relation is nonlinear as in Equation (3.3) (Kenneth G. McConnell, 2008).

$$F = (B_0.l.n)\left[1 - \left\{\frac{x + x_0}{x_{\max}}\right\}^2\right] I \tag{3.3}$$

However, if the shaker stroke is centered well $(x_0 = 0)$ and the motion x is small with respect to $x_{\max}$, Equation (3.3) is considered to be linear for many practical cases. (Kenneth G. McConnell, 2008)

According to Lenz law, induced voltage (back emf) in the voice coil is related to the velocity of the voice coil as in Equation (3.4) (Kenneth G. McConnell, 2008).

$$E_{bemf} = (B.l.n)\dot{x} = (B_0.l.n)\left[1 - \left\{\frac{x + x_0}{x_{\max}}\right\}^2\right]\dot{x} = k_2\,\dot{x} \tag{3.4}$$

As in Equation (3.3), for large level of motion nonlinear behaviour exists for E_{bemf} & velocity relation, too and k_2 in Equation (3.4) is E_{bemf} & velocity constant.

3.4 Power Amplifiers

As the operation of power amplifiers are beyond the scope of this study, a brief information is introduced in this section.

There are two modes of operation for power amplifiers as current and voltage modes. Basic schematic mode can be found in (Kenneth G. McConnell, 2008).

The shaker which we used for this study was driven by a voltage mode power amplifier. The power amplifier modifies the controller's drive voltage signal $V(\omega)$ by multiplying with the gain value $G(\omega)$ in order to have required voltage level $E(\omega)$. In frequency domain ω, the relation is as in Equation (3.5) (Kenneth G. McConnell, 2008).

$$E(\omega) = G(\omega).V(\omega) \tag{3.5}$$

For well designed shakers, $G(\omega)$ is a constant value throughout the shaker frequency range.

CHAPTER 4

RANDOM VIBRATION TESTS

The vibration type, which is encountered in real life applications, is neither periodic nor predictable and it is called as random vibration. Therefore, random vibration tests are performed by environmental test labs which expose the UUT to real life conditions in order to check for failures prior to usage on site.

In contrast to sinusoidal vibration tests which create single frequency excitation at any time of the test duration, random vibration tests excite the UUT at all frequencies of the test spectrum simultaneously at any time of the test. It means that resonances of the UUT, which are within the test frequency range, are excited at the same time in random vibration tests, thus real environmental conditions can be simulated better by this type of test for pass/fail detection.

In this chapter, The demanded random vibration test profile of this study is introduced with aborted test results. Estimation of signal rms values by using PSD data is explained which is used in Chapter 5 to obtain FRF of the electro-dynamic shaker in acceleration/voltage. Besides, possible errors which can be seen during a random vibration test and different control strategies are explained which are expected to be useful for test engineers.

4.1 The Random Vibration Test Profile

During a random vibration test, random signals are generated and controlled. The signals are compatible with gaussian amplitude characteristics and have special spectrum shapes.

A random vibration test profile is defined by acceleration power spectral density (PSD) and fast fourier transform (FFT) technique is used to measure test profile PSD during the random vibration test. In Figure 4.1, a random vibration test profile can be seen with tolerances which are according to some test standarts such as MIL-STD-810G. The test profile excites the test item at the frequencies from 20 Hz to 2000 Hz. Frequency resolution is a parameter for test setup software and it divides the frequency range to define control frequencies during the test. Yellow lines in the profile indicates the acceptable vibration level during the test. If the controlled random signal is between these two yellow lines, the test is considered to be successful. If the controlled random signal is between yellow and red lines, it is said that there is excessive vibration at those frequencies but the test still continues. If the controlled random signal exceeds red lines, the vibration level is very high as more than four times higher than the real profile vibration level and test is aborted. Vibration test profile breakpoints and tolerance levels are seen in Table 4.1.

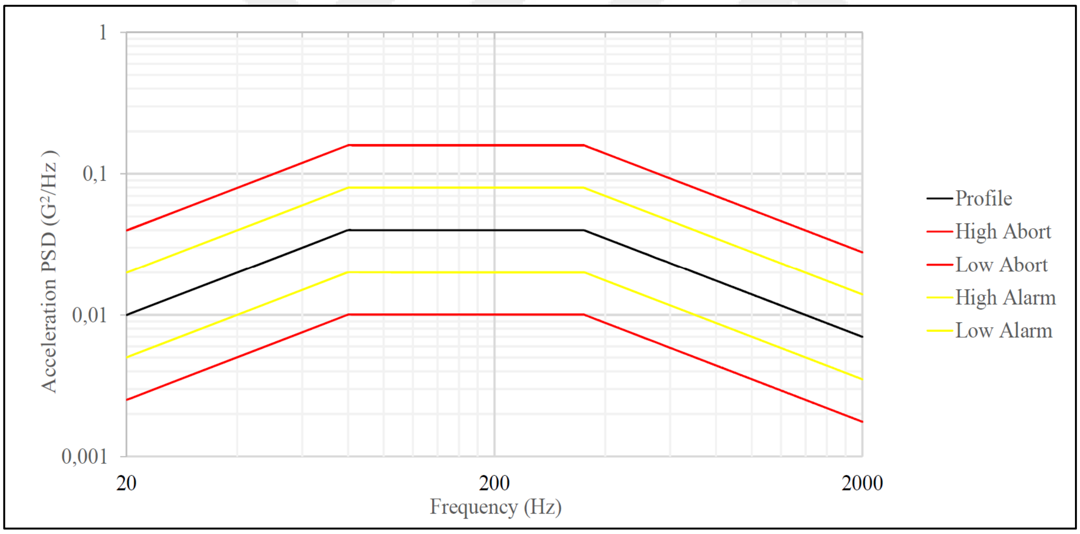

Figure 4.1. A vibration test profile

Table 4.1 Vibration test profile break points and tolerances

Frequency (Hz)	*Acceleration PSD (g^2/Hz)*	*High Abort (dB)*	*High Alarm (dB)*	*Low Alarm (dB)*	*Low Abort (dB)*
20	0.01	6	3	-3	+6
80	0.04	6	3	-3	+6
350	0.04	6	3	-3	+6
2000	0.007	6	3	-3	+6

The unit of acceleration PSD is g^2/Hz and g stands for gravitational acceleration. The area under the acceleration power spectral density profile indicates the power or mean square of the signal which is the square of signal root mean square (rms) value. Peak acceleration level which can be reached during a random vibration test can be estimated by gaussian amplitude statistics. When the signal has a zero mean value (it is valid for all random vibration profiles), acceleration rms value (g_{rms}) is equal to standart deviation, σ. ±3σ covers the 99.73% of the probability distribution function which means that ±3 g_{rms} is the peak acceleration level for 99.73% of the total test time which is a good estimation to use for proper shaker load capacity selection.

4.1.1 Estimation of the Peak Amplitude at a Test Frequency

Summation of sine series can be used for generating pseudo acceleration signal as in Equation (4.1) (Rice, 1944).

$$a(t) = \sum_{i=1}^{N} \sqrt{2S_a(\omega_i)\Delta\omega}\,\sin(\omega_i t + \phi_i) \tag{4.1}$$

where the Power Spectral Density was divided by N frequency intervals $\Delta\omega$, and the phase angles ϕ_i are random values for each center frequency band ω_i , so the process is supposed to be a superposition of sine periodical signals with uncorrelated phase angles. As we investigate the equation, we can conclude that for each center frequency ω_i , $\sqrt{2S_a(\omega_i)\Delta\omega}$ term is the amplitude of the corresponding signal where $S_a(\omega_i)$ is the auto acceleration PSD in g^2/Hz. One can also make this conclusion as voltage PSD and pseudo voltage signal as in Equation (4.2).

$$e(t) = \sum_{i=1}^{N} \sqrt{2S_e(\omega_i)\Delta\omega} \sin(\omega_i t + \phi_i) \tag{4.2}$$

In Equation (4.8), $S_e(\omega_i)$ is the auto voltage PSD in V^2/Hz. However, Fast Fourier Transform is used by modern shaker controllers to measure PSD data. In order to eliminate spectral distortions due to the signal & analyzer asynchronism, a windowing function called Hanning Window is usually used. Thus, 1.5 is used instead of 2 in signal amplitude expressions.

4.1.2 Control Algorithm for Random Vibration Test

During a vibration test, control system of the vibration test system drives the shaker and investigate the actual produced excitation level. If the actual excitation level is out of tolerance limit of the reference (desired) level, drive signal is adjusted to put real excitation levels within the limits. In order to achieve accurate control, control system continuously corrects the dynamics of the test setup load in real time.

A closed loop random vibration control block diagram of a commercial electro-dynamic shaker can be seen below. Control signals, which indicate the response of the UUT, are collected by accelerometers. A random controller is continuously produce drive signal to adjust the PSD of the control signal with respect to reference PSD signal (test profile) within the test tolerances.

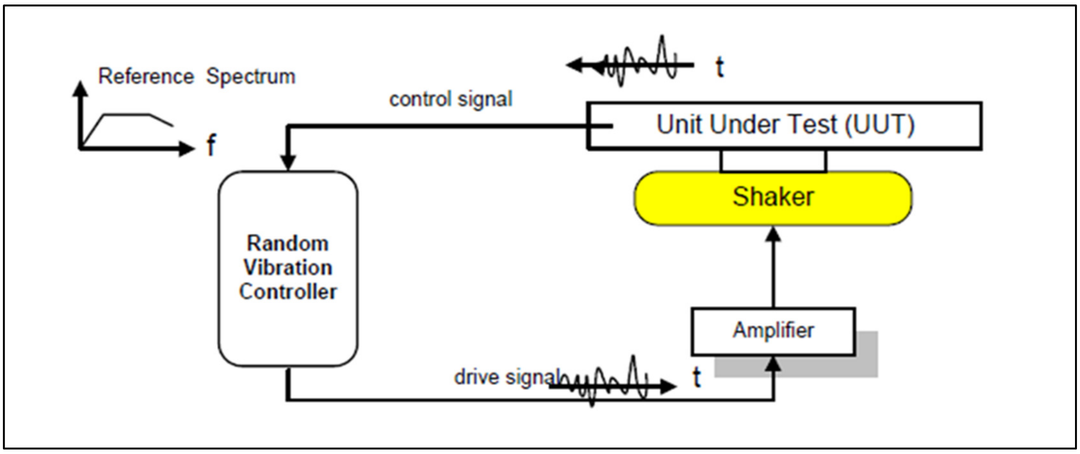

Figure 4.2. Vibration Controller block diagram (LDS DACTRON, 2008)

4.1.3 Possible Errors occur during a Random Vibration Test

There are four possible errors which can be arisen during a random vibration test and they can cause the test to abort. In a random vibration test, these errors can be seen individually or in combination and they are summarized in the following sections.

4.1.3.1 Noisy Measurement

When the drive voltage signal levels at some center frequencies drop below the noise threshold level of the test system, the test cannot be controlled at those frequencies and the test is aborted. This type error is mostly seen when the acceleration levels during a random vibration test is very low. In this case, controller produces very weak drive signals around noise threshold level which makes the control unstable.

4.1.3.2 High g_{rms}

When the controlled signal mostly stays within the tolerance band of the random vibration test profile, there can be some resonant regions which cannot be controlled adequately. Due to the fact that the controlled signal level is greater than random vibration test profile at these regions, the total g_{rms} of the controlled signal or in another words the area under the controlled signal is greater than the total g_{rms} of the random vibration test profile. If the abort limit of the total g_{rms} of the random vibration test profile is exceeded, test is stopped. In Figure 4.3, the aborted test profile of the case study is seen. Beyond 600 Hz, control signal diverges from the test profile.

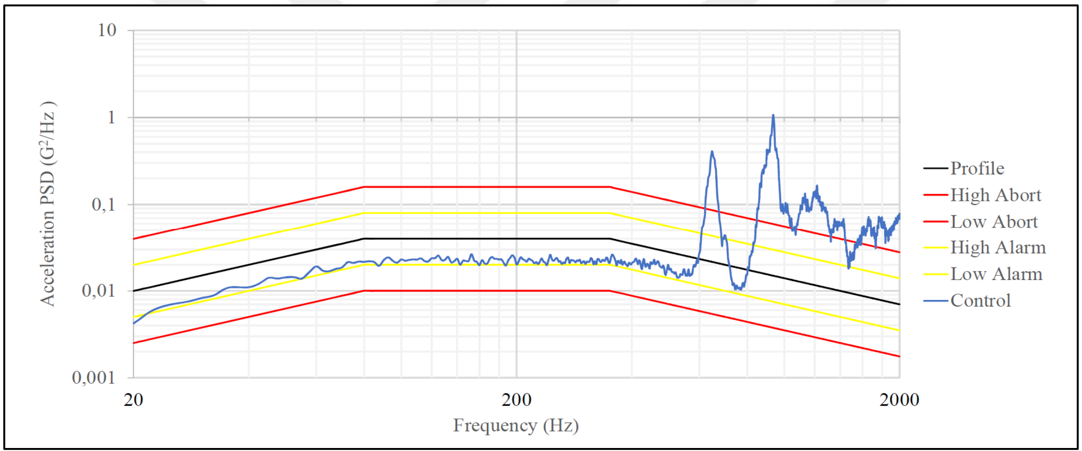

Figure 4.3. Aborted real test

4.1.3.3 Overload of Control Accelerometer(s)

During a random vibration test, control accelerometers can be overloaded due to high level test profile or severe resonant regions occur during the test. When the limits of accelerometers are exceeded, related error message which indicates problematic accelerometer/s can be seen and the test is aborted.

4.1.3.4 High Line

If the number of center frequency lines which are out of the abort limit exceed a defined ratio of whole frequency lines, test is aborted. In Figure 4.3, the error message was about high line error because of steep peaks around 650 Hz and 935 Hz.

4.1.4 Control Strategies for a Proper Random Vibration Test

Modern controllers of electro-dynamic shakers present several control techniques. The most suitable technique should be chosen according to test setup.

Single channel control method uses just one accelerometer to control the vibration level with respect to real vibration profile.

Weighted average control method uses multiple control accelerometers depending upon the controller capacity. According to test conditions, weighting of the each accelerometer can be adjusted. Equal weighting is used by default.

Maximum control method checks the vibration level at each center frequency for all control accelerometers and produce a composite control signal according to the largest vibration levels.

Minimum control method checks the vibration level at each center frequency for all control accelerometers and produce a composite control signal according to the lowest vibration levels.

The objective of a vibration test is to excite the UUT at desired vibration levels. If there is a resonant behaviour exist because of the structure of vibration test fixture, it is very important where the control accelerometers are located. In general, control accelerometers are located as close as possible to vibration test fixture & UUT mounting interface. If multiple mounting locations exist and there is a resonant behaviour of the vibration test fixture, none of control methods can eliminate the resonant behaviour. The control methods try to optimize the vibration level at acceleration mounting points, resonance or anti-resonance behaviour can be seen at any other points on fixture & UUT interface.

In order to avoid confusion and possible errors during a vibration test, vibration test standards are written which include procedures and practical approaches for vibration tests. One of these standards is MIL-STD-810 Revision G. Although the standard leaves the most problematic issues to the test conductors, important keynotes about vibration test control are as follows:

Control accelerometers must be mounted on the vibration test fixture next to UUT mounting points.

Test tolerances are defined as ±3 dB for test frequencies below 500 Hz, and ±6 dB for test frequencies above 500 Hz. If these tolerances can not be met due to physical limitation, tolerances can be increased at minimum attainable level which is authorized by test engineers and customers. Regions where the tolerance is increased must be maximum 5% of total test frequency band. If not, test method, vibration test fixture or facility must be changed in order to meet tolerance requirements.

CHAPTER 5

DEVELOPMENT AND DEMONSTRATION OF THE RESONANT VIBRATION PROBLEM SOLUTION METHOD FOR THEPROBLEMATIC VIBRATION TEST FIXTURE

In this chapter, the problematic UUT, vibration test fixture, shaker assembly and random vibration test scenario is introduced. In order to understand dynamic characteristics of the shaker being used in the test and all test configurations, several vibration tests are conducted and presented in this chapter. A reasonably accurate dynamic model of the whole test setup is established by using a commercial finite element analysis software. In order to reduce vibration levels around resonance frequencies of UUT, vibration test fixture, shaker assmebly, damping increase is presented as a potential solution. The proposed method is using viscoelastic material based tuned vibration absorbers (TVAs) tuned to problematic resonant frequencies. Various TVAs are tuned properly and physically applied to the UUT, vibration test fixture assembly to solve the problem of random test aborting due to practical method to add damping to the test setup is applied.

5.1 Description of the Problematic Random Vibration Test Scenario

A previously designed vibration test fixture was intended to perform random vibration tests on a specific UUT along three test directions. There was a design constraint on the vibration test fixture that the shaker being used can only be operated in vertical configuration for all three test directions due to the lack of a slip table. Due to this constraint, it was intended that test configurations along all test directions are just achieved by making simple assembly modifications of the vibrations test fixture on the shaker in its upright orientation. For this particular test application, not only there was no means to make an extra investment for a slip table in order to perform tests in horizontal directions but also it was also decided that use of a slip table would be time consuming work to reconfigure the test system. The latter advantage of the vibration test fixture results less labor need, thus labor costs are decreased. On additional constraint was to minimize the total mass of the UUTs and the vibration test fixture due to limits coming from the shaker capacity. Shaker capacity introduced a total mass limit of about 40 kg .

Additionally, the current design makes it possible to perform vibration tests of two UUTs at the same time along all test directions by using this test fixture. In Figure 5.1, problematic test direction of the vibration test fixture is seen. Rotation of the UUTs by an angle of 90 degrees, provides the second axis for testing which is also problematic, that is the intended random vibration test can not be performed because the shaker controller system aborts the test due to excessive resonant vibrations observed in the control acceleration data. The third and the last axis of testing of the UUTs is seen in Figure 5.2. This configuration is more rigid than the problematic configuration and the desired random vibration profile can be obtained.

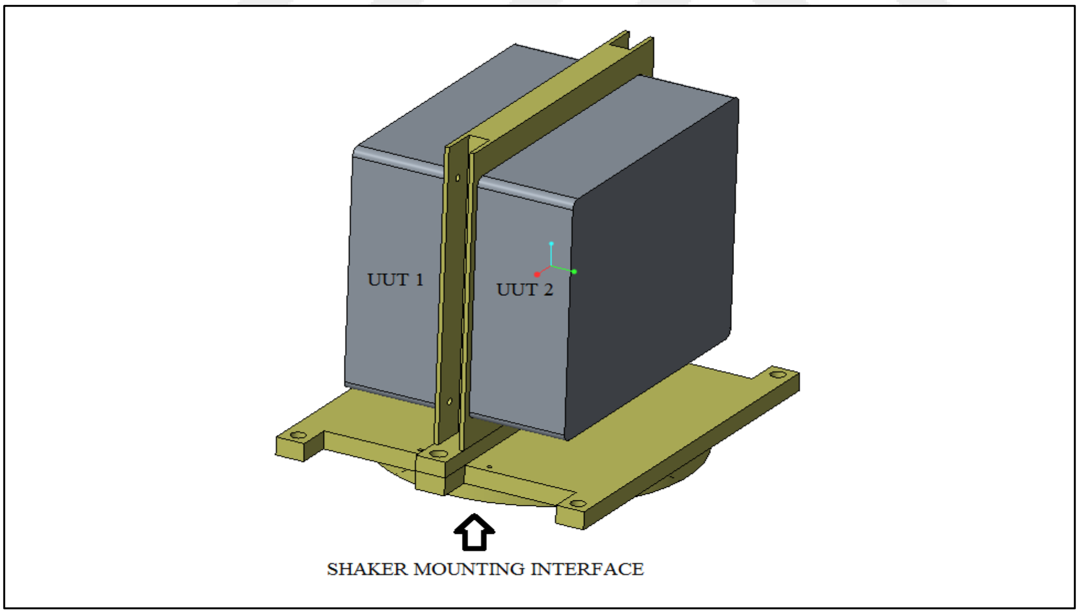

Figure 5.1. Vibration test fixture configuration in Z direction with 2 UUTs

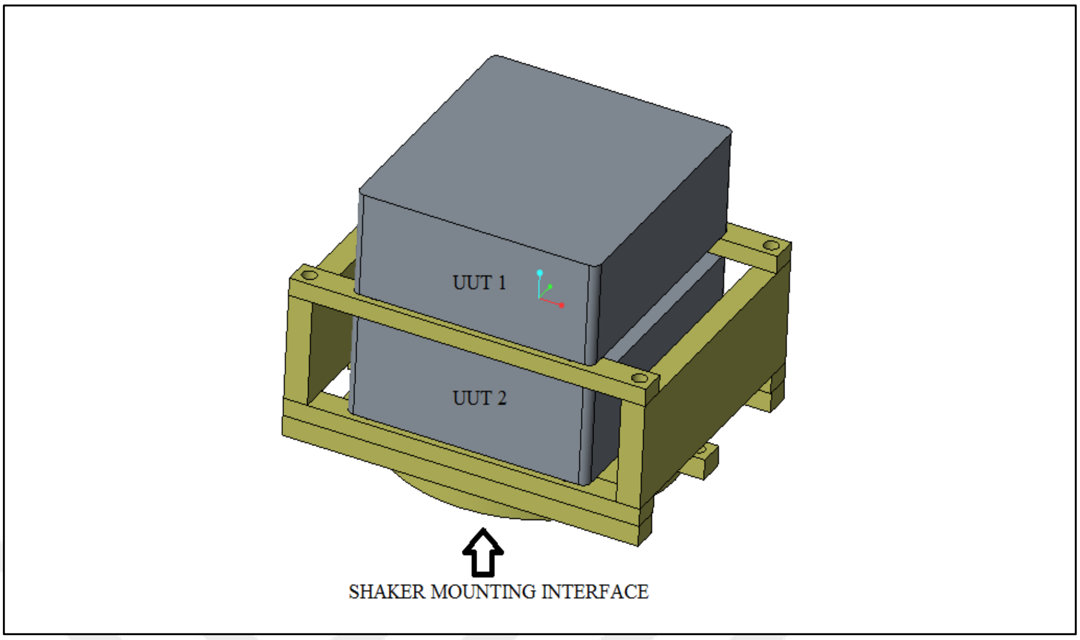

Figure 5.2. Unproblematic vibration test fixture configuration

The vibration test fixture parts are manufactured by traditional machining processes. Parts are assembled together by proper bolts because simple assembly reconfigurations are required for test axis orientation. A commercial aluminum alloy is used for fabrication which is readily available in markets with affordable prices.

In this thesis actual UUTs are not used due to these products containing proprietary information. Instead of using real UUTs, dummy UUTs are designed which have equivalent mass and inertia values and overall dimensions same as the real UUT. Dummy UUT without the cover component can be seen in Figure 5.3. Four mounting holes at the corners are used for assembling UUT to vibration test fixture. The mass of the vibration test fixture is within the limits for performing vibration tests according to vibration test profile, dummy masses and shaker load capacity.

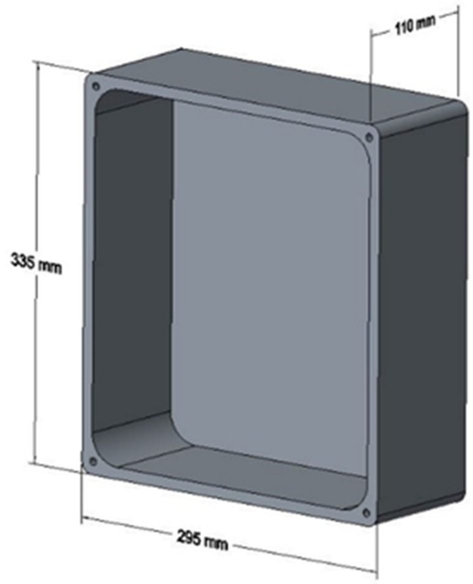

Figure 5.3. Dummy UUT

The actual UUT test configuration where the vibration test fixture which is adjusted for the problematic horizontal direction (along gravity) can be seen in Figure 5.4 and Figure 5.5. In Figure 5.4, total test setup is seen which includes electro-dynamic shaker, adapter plate, vibration test fixture and two UUTs. Figure 5.5 is a closer view of Figure 5.4 for clarifying accelerometer mounting points. In Figure 5.5, the bottom plate of the vibration test fixture has 2 threaded holes for mounting control accelerometers. The place of the holes are chosen as close as one of the bottom mounting hole of the UUT due to the fact that the UUTs are excited from their mounting holes.

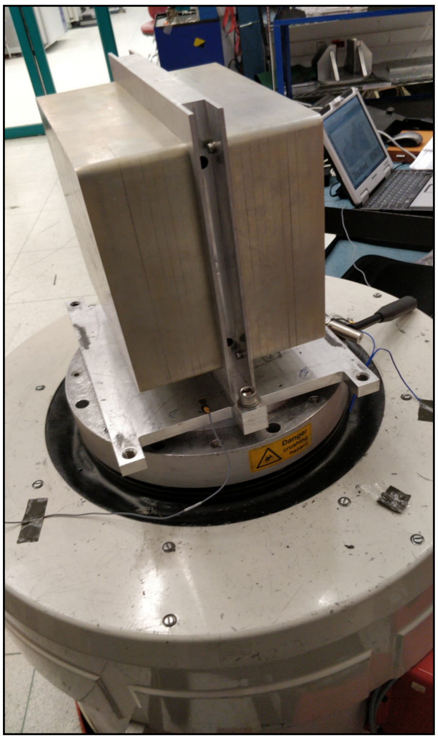

Figure 5.4. Real test setup

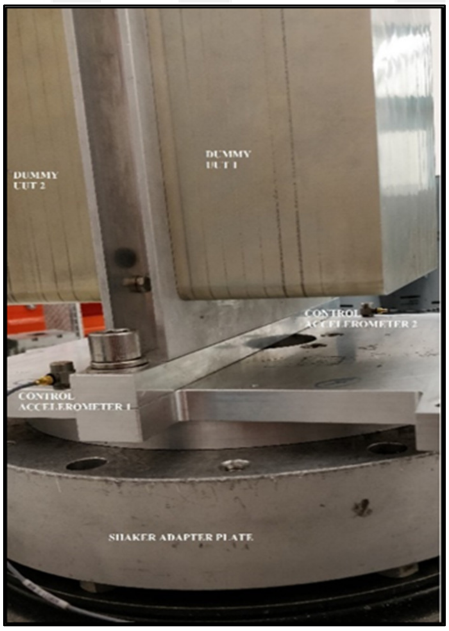

Figure 5.5. Real test setup (closer view)

In order to control resonant regions better at two control points, weighted average method is chosen for control algorithm. The desired test profile which is seen in Figure 5.6 is entered in the shaker controller interface by using the breakpoints in Table 5.1.

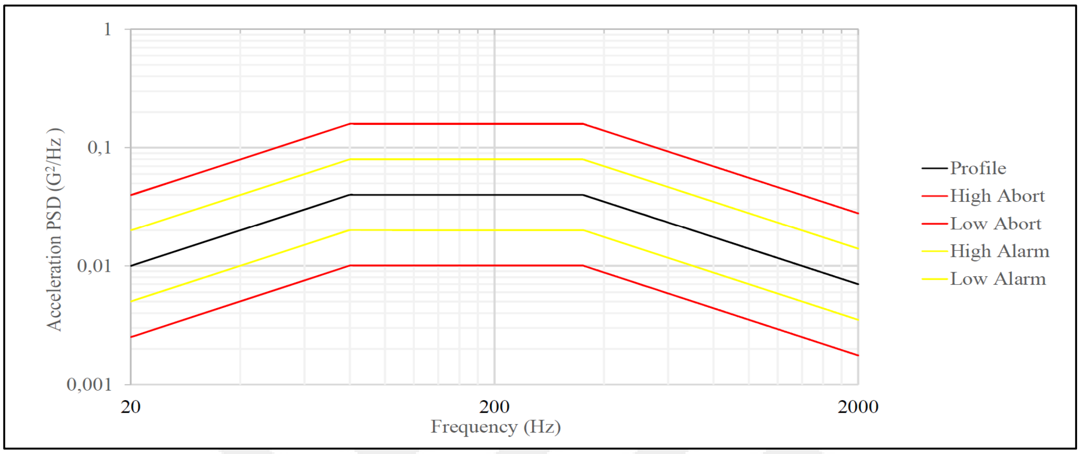

Figure 5.6. The desired random vibration test profile

Table 5.1 Breakpoints and tolerances of the desired vibration test profile

Frequency (Hz)	*Acceleration PSD (g^2/Hz)*	*High Abort (dB)*	*High Alarm (dB)*	*Low Alarm (dB)*	*Low Abort (dB)*
20	0.01	6	3	-3	+6
80	0.04	6	3	-3	+6
350	0.04	6	3	-3	+6
2000	0.007	6	3	-3	+6

After all required test preparations, the vibration test is started. However, the test is aborted at a pre-test (50% energy level of the real profile) step due to severe resonant behavior of the test setup. The error message which is arisen in controller's screen is a high line error as it is seen in Figure 5.7. In addition, Figure 5.8 shows the aborted test before reaching the desired test profile.

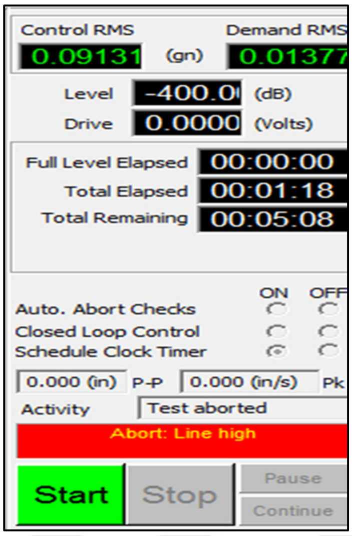

Figure 5.7. Error message given by the shaker controller software fort the aborted test

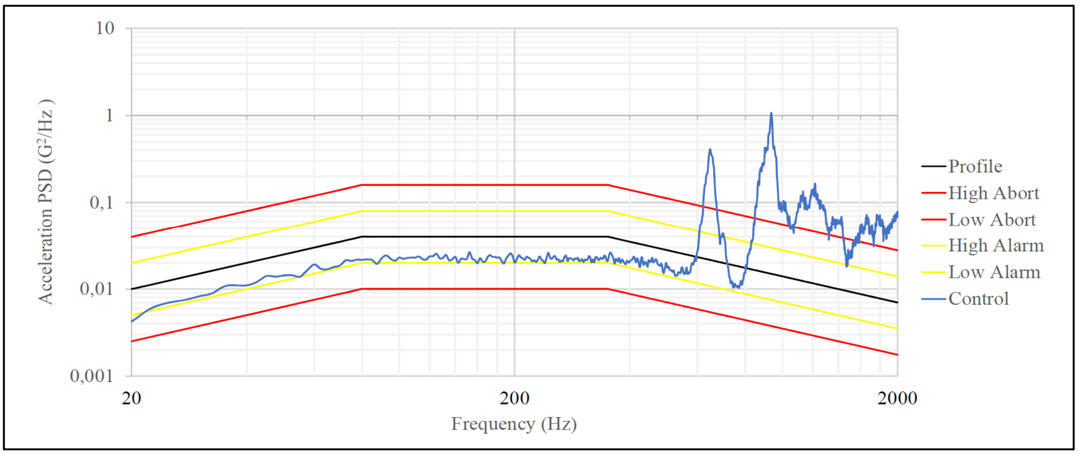

Figure 5.8. Aborted test profile for the problematic vertical test configuration

An alternative test was performed in order to investigate the dynamics of the problematic test configuration at the original control accelerometer mounting locations. An additional control accelerometer was mounted on the armature table for this alternative test. Now for this test, two monitor accelerometers were located at the same places where the control accelerometers of the aborted test are located as they can be seen in Figure 5.9. The alternative test is conducted to estimate acceleration transmissibility functions between the shaker armature and the control acceleration locations of the problematic test configuration.

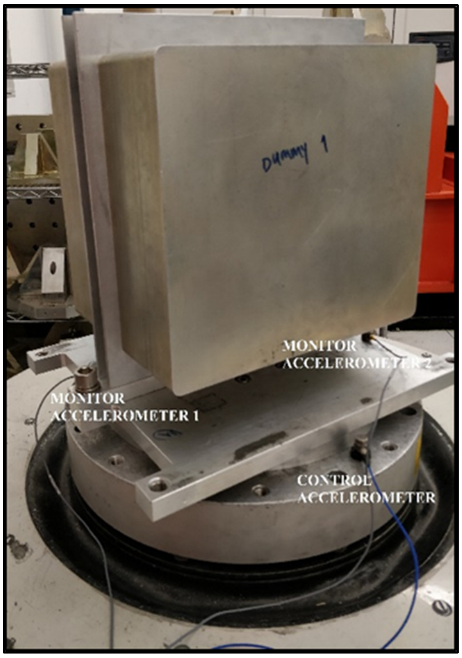

Figure 5.9. The alternative test setup for transmissibility Estimation

A 0.001 g^2/Hz white noise random vibration profile is applied along the original test frequency bandwith for the alternative test. Due to symmetry of the test setup and monitor accelerometer locations, transmissibility values acquired through the alternative test between the control accelerometer and the monitor accelerometers are similar. Transmissibility plot of one of the monitor acceleration locations on the vibration test fixture abtained the alternative test is seen in Figure 5.10 and this plot is later going to be used to validate FE model of the whole test setup. After validating FE model, peaks in tranmissibility plot of the FE model are compared with peaks in the aborted random vibration test profile and problematic modes are identified one by one.

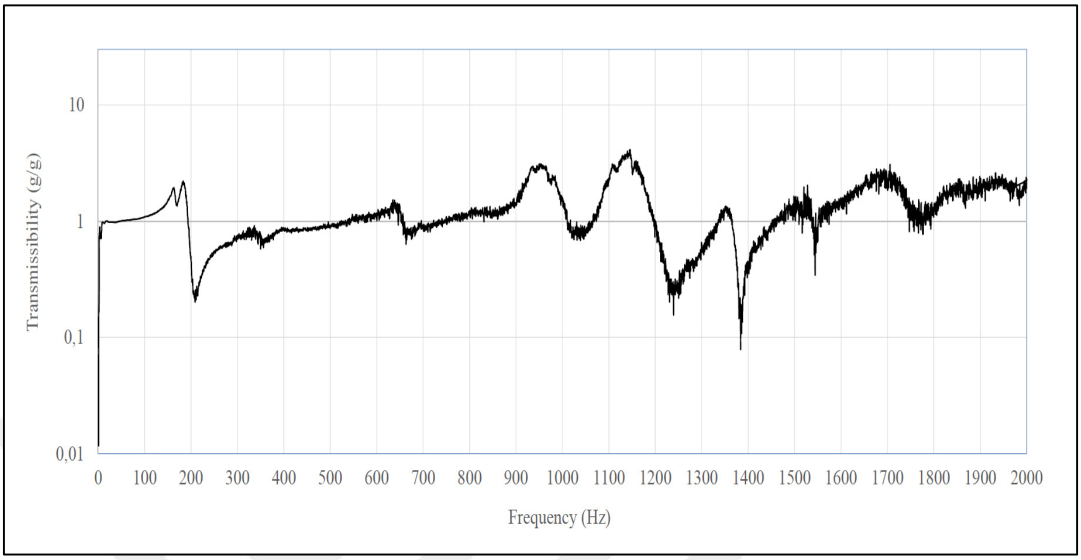

Figure 5.10. Transmissibility plot obtained from the the alternative test (Input location is the shaker armature. Output location is the monitor accelerometer 1 on the vibration fixture plate.)

5.2 Finite Element Modeling of the Test Setup

In this section, finite element model of the test setup is generated which will also include the shaker dynamics. However, only the mechanical model of the shaker is going to be available in the light of available shaker information as it will be discussed in the next part of this section. After modeling of the shaker which is used during test, models of the vibration test fixture and dummy UUTs are mounted to the shaker model in order to correlate and verify the whole test setup model to actual system setup using measured transmissibility plot shown in Figure 5.10, which is obtained by performing the alternative test.

5.2.1 Finite Element Modeling of the Shaker

As it is discussed in Chapter 3, dynamic model of a shaker is a coupled model in which mechanical force, electrical current, mechanical velocity and electrical voltage are interrelated. In order to understand how current and voltage change with respect to frequency, a one degree of freedom model is analyzed with electrical model (Kenneth G. McConnell, 2008). This model is also valid until the half of the armature resonance frequency because accelerance of the table (where the vibration test fixture and test item are mounted) due to a forcing at table and accelerance of the table due to a forcing at coil are the same till the half of the armature resonance frequency, in another words table and coil move as a rigid body till that frequency (suspension mode). In addition, isolation mode resonant behaviour is not severe. Thus, isolation mode is also out of concern for the model in Figure 5.11.

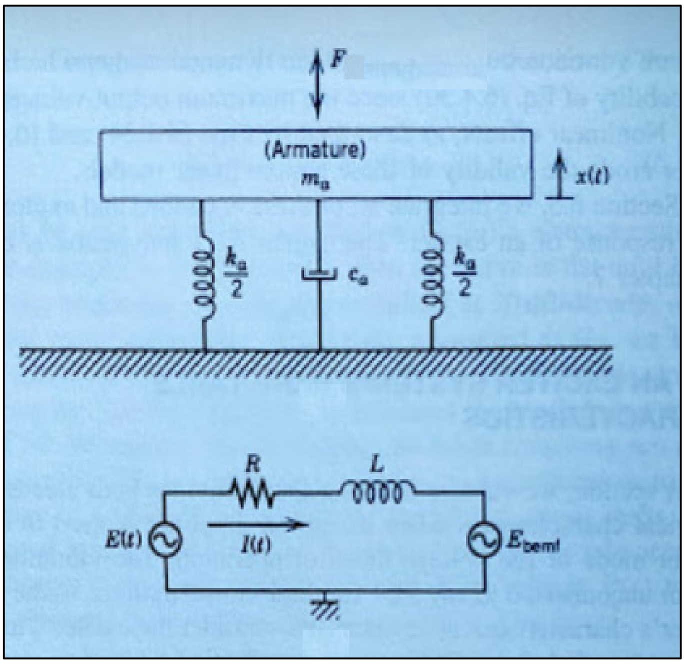

Figure 5.11. One DOF armature model with electrical model (Kenneth G. McConnell, 2008)

Governing differential equations of the models in Figure 5.11 are presented as Equation (5.1) and Equation (5.2) :

$$m_a \ddot{x} + c_a \dot{x} + k_a x \ = \ F(t) \ = \ k_1 I(t) \tag{5.1}$$

$$RI + L\dot{I} + E_{bemf} = RI + L\dot{I} + k_2 \dot{x} = E(t) \tag{5.2}$$

In Equation (5.1), m_a is the total mass of the armature which is the sum of table and armature masses, k_a and c_a are armature stiffness and damping respectively. $F(t)$ is the force created in the coil and k_1 is the linear force & current constant.

Equation (5.2) shows the relation between input voltage $E(t)$, currrent and velocity in which R is the coil resistance, L is the coil inductance and k_2 is the linear voltage & velocity constant.

For a constant accelerantion test, reference phasor is the displacement $x(t) = Xe^{j\omega t}$. Current and voltage change with respect to frequency can be derived by using Equation (5.1) and (5.2).

$$\left(\frac{-k_a}{\omega^2} - m_a + \frac{jc_a}{\omega} \right) \left(-\omega^2 X \right) = k_1 I_0 \tag{5.3}$$

In Equation (5.3), $\left(-\omega^2 X \right)$ term and k_1 are constants. Thus, current change with respect to frequency can be plotted by knowing shaker parameters.

In addition, voltage change with respect to frequency can be derived as in Equation (5.4) in which $\left(-\omega^2 X \right)$ term, k_1 and k_2 are constants.

$$\left(\frac{-Rk_a}{\omega^2 k_1} + \frac{Rm_a}{k_1} + j\frac{Rc_a}{\omega k_1} - j\frac{Lk_a}{\omega k_1} + j\frac{L\omega m_a}{k_1} - \frac{Lc_a}{k_1} - j\frac{k_2}{\omega} \right) \left(-\omega^2 X \right) = E_0 \tag{5.4}$$

As we mentioned earlier, shaker parameters are needed to plot the changes. However, all required shaker parameters are not available information due to confidential issues. Parameters of a modal shaker which are available in Kenneth G. McConnell (2008) will be used to make plots. In Figure 5.12, current change with respect to frequency is seen. The current is at the lowest value at the resonance frequency (around 400 Hz) of the armature which means that force requirement is at the lowest value in order to obtain constant acceleration level. It is nothing but the resonance characteristics of the mechanical system.

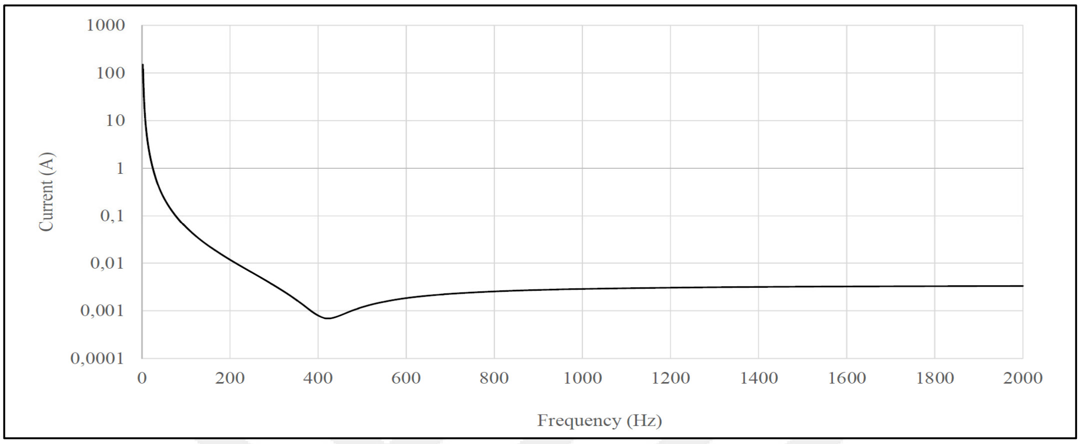

Figure 5.12. Current change for constant acceleration for the shaker model developed by Kenneth G. McConnell (2008)

In Figure 5.13, voltage change with respect to frequency is seen. Note that, voltage change is depended on current and velocity at the same time. Up to the resonance frequency, voltage change rate is high because of reducing current (force) need around the resonance. After the resonance region which means that higher frequency region, current (force) need converges to a constant level. At higher frequencies, velocity level is lower for constant acceleration. Thus, voltage required in order to obtain a velocity level at high frequencies is lower than the voltage required in order to obtain the same velocity level at lower frequencies obtain a velocity level at high frequencies is lower than the voltage required in order to obtain the same velocity level at lower frequencies.

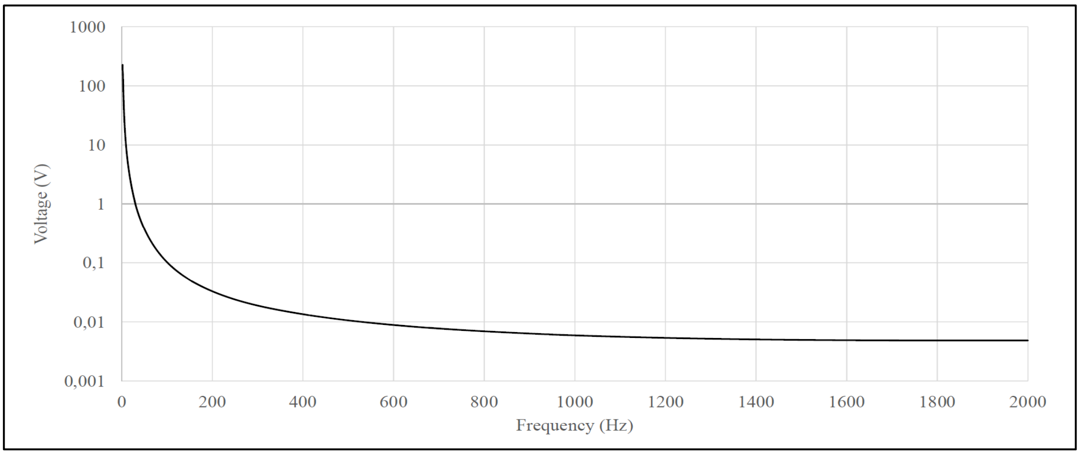

Figure 5.13. Voltage change for constant acceleration for the shaker model developed by Kenneth G. McConnell (2008)

In Figure 5.14, voltage/current change with respect to frequencies is seen. For the lower frequencies and higher frequencies region, voltage/current ratio can be considered as constant except the resonance region.

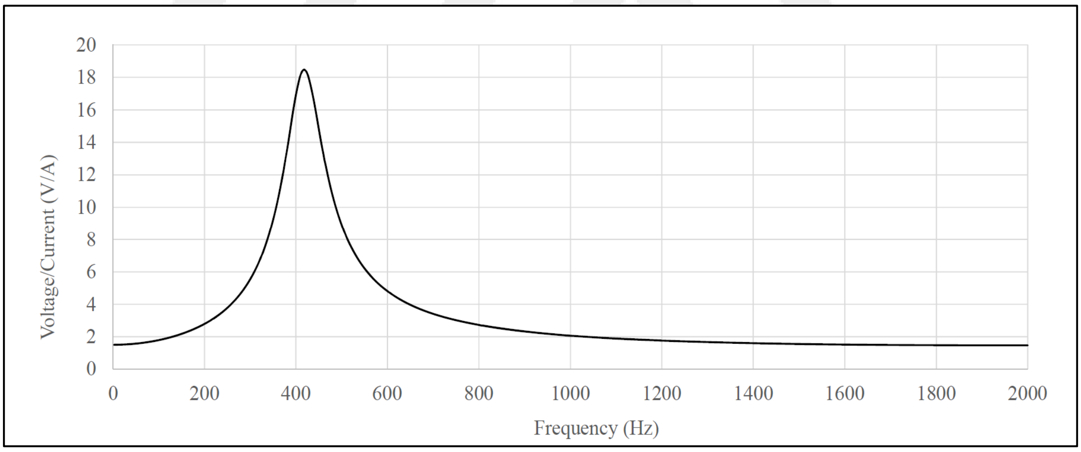

Figure 5.14. Voltage/Current change for constant acceleration for the shaker model developed by Kenneth G. McConnell (2008)

In order to obtain experimental data of the actual shaker used in the problematic test fixture, a constant acceleration test is performed on the shaker armature without the vibration test fixture and the UUTs. A 0.02 g^2/Hz white noise random vibration profile is applied in the the original test frequency bandwith (20-2000 Hz) using a control accelerometer on the armatüre as seen in Figure 5.15. Drive voltage PSD and control acceleration PSD are available through the controller software as the test outputs of a random vibration test.

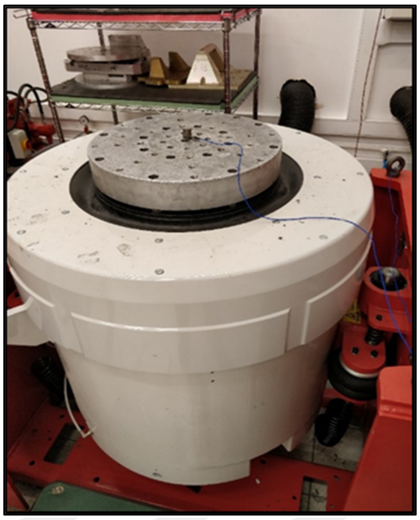

Figure 5.15. Random vibration test configuration: shaker without the UUTs and the vibration test fixture

Drive voltage PSD information is used to calculate RMS voltage level for each center frequency by using Equation (4.2). Voltage RMS change versus frequency plot for the white noise test perfomed on the shaker is seen in Figure 5.16. Characteristic of the Figure 5.16 is similar to Figure 5.13 for the lower frequencies where the suspension mode is dominant. On the other hand, isolation mode is around 3-5 Hz as it is specified in shaker catalogue and it is out of test frequency bandwith. In addition, resonant behaviour is not severe. However, the most critical mode of the shaker is the armature mode which occurs at high frequency region and the armature resonant frequency is seen as the frequency at the lowest point of valley. As it is discussed earlier voltage need is much more lower at higher frequencies for the velocity need of a constant acceleration test. Current (force) need is also decreased due to armature resonance behaviour at higher frequencies.

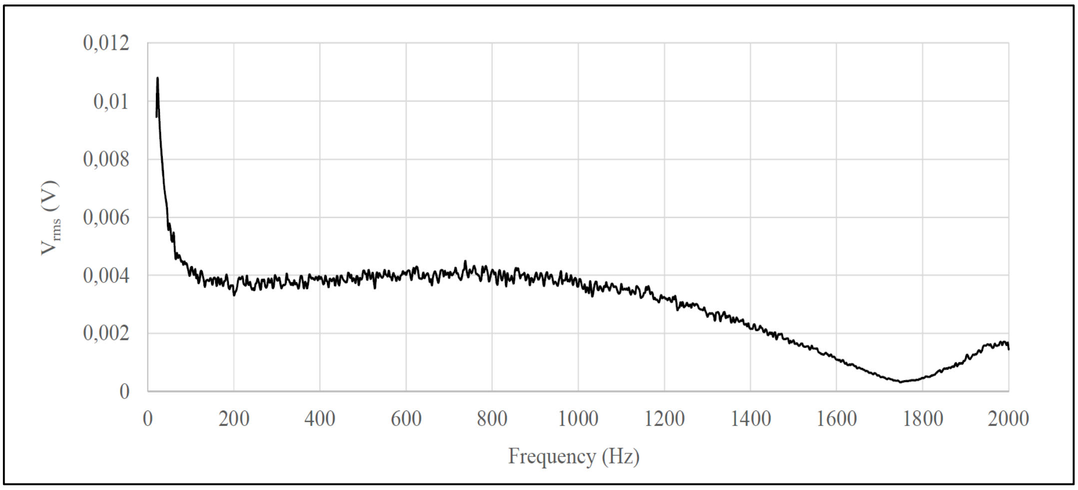

Figure 5.16. V_{rms} plot for the white noise test

By investigating Figure 5.16, it is found that armature resonance occurs around 1782.5 Hz. In addition for a centered stroke with respect to payload, suspension mode remain unchanged. For the shaker in use, suspension resonant frequency is around 100 Hz in catalogue and it is also verifed by a hammer test by using the same test setup as in Figure 5.15.

Figure 5.8 shows the realized PSD and the target PSD plots of the aborted test and it is seen that the control signal follows the demanded vibration profile till 600 Hz. Thus, adverse effects of the suspension mode is seemingly handled by the shaker controller. It is concluded that it is adequate to model only armature mode of the shaker as two lumped masses connected to each other by spring and damping elements. Moving mass of the armature is given as 32.9 kg in the shaker catalogue and mass of the aluminum alloy adapter plate present of the orginal shaker armature top plate is 28 kg. At this point a reasonable approach is made to transfer the available test FRF from g/V unit to ms^{-2}/N. After this conversion, FE model can be adjusted according to test FRF. By investigating Figure 5.14, after three times of suspension resonant frequency, voltage /current ratio is considered to be constant. Suspension resonance of the shaker is 100 Hz and the voltage level at 300 Hz will be used to make derivations.

For a successfully completed random vibration test, FRF estimation as acceleration per volt can be stated as in Equation (5.5).

$$S_a(\omega_i) = \left| H(j\omega_i) \right|^2 S_e(\omega_i) \tag{5.5}$$

In Equation (5.5), $S_a(\omega_i)$ is the auto acceleration PSD in g^2/Hz, $H(j\omega_i)$ is the FRF in g/V, ω_i is the frequency, j is the imaginary number and $S_e(\omega_i)$ is the auto voltage PSD in V^2/Hz. By using unloaded shaker PSD information, FRF plot of the empty shaker is seen in Figure 5.16.

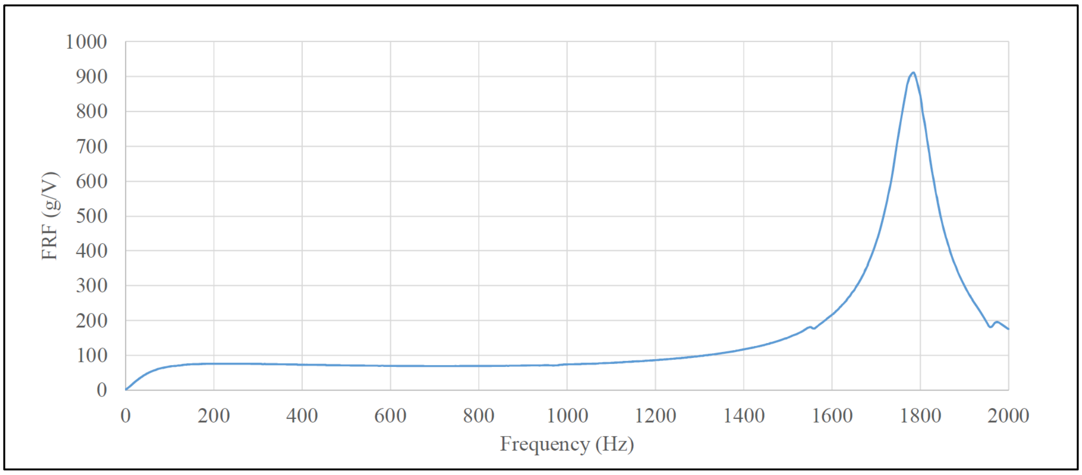

Figure 5.17. FRF plot of the unloaded shaker test in g/V

FRF value is 76.44 g/V at 300 Hz and at this frequency our armature model behaves as a rigid mass which is the sum of armature moving mass and adapter plate (60.9 kg). For 1 g acceleration, 597.2463 N is required by applying Newton's Second Law and 1/76.44 V creates this acceleration. Hence, the ratio between voltage and force is 45653.51 N/V. If we divide FRF values in g/V by 45653.51 N/V and multiply by 9.807 m/s^2, we find shaker FRF in ms^{-2}/N and it is plotted as in Figure 5.18.

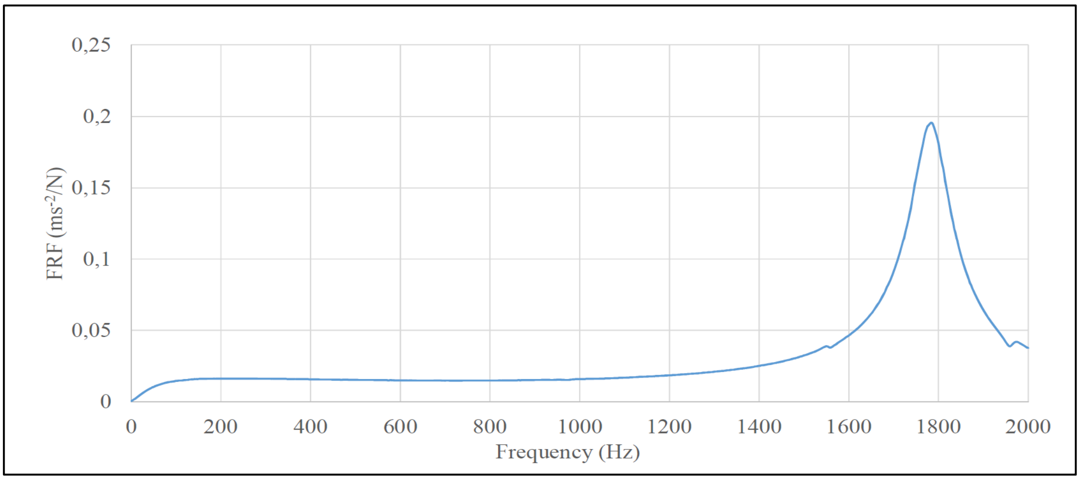

Figure 5.18. FRF plot of the unloaded shaker test in ms^{-2}/N

Total moving mass of the armature is divided equally for coil mass and table mass as 16.45 kg, respectively. Then, adapter plate is mounted on the table mass side. Appropriate spring and damping values are found by trial and error method and tabulated in Table 5.2 in order to obtain armature resonance frequency and FRF value at the resonance frequency. Note that, shaker model has two modes, rigid body mode and armature mode. In harmonic analysis of the FE model, force is applied to coil mass and acceleration on the adapter plate is measured. In Figure 5.19, FRF plots from test and FE model are seen. Two plots do not perfectly match due to velocity effect in voltage.

Table 5.2 Coefficients of the shaker FE model elements

Lower Mass (kg)	*Upper Mass (kg)*	*Spring Coefficient (N/mm)*	*Damping Coefficient (N.s/mm)*	*Mass of Adapter Plate (kg)*
16.45	16.45	1530075.1	11.5	28

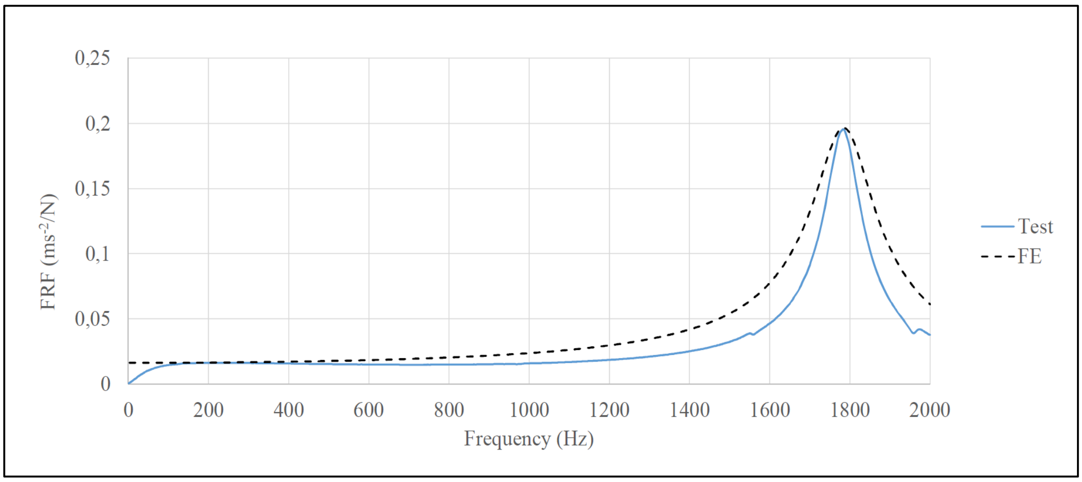

Figure 5.19. Shaker FRF plot comparison, test & FE models

Shaker FE model is seen in Figure 5.20 and shaker FE model with adapter plate is seen in Figure 5.21.

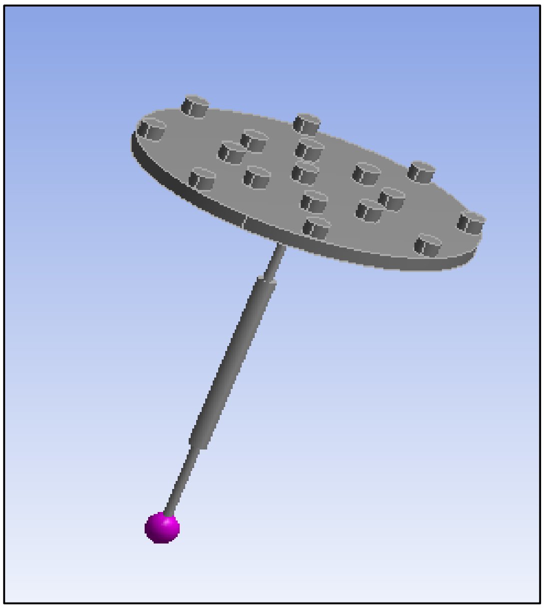

Figure 5.20. Shaker FE model

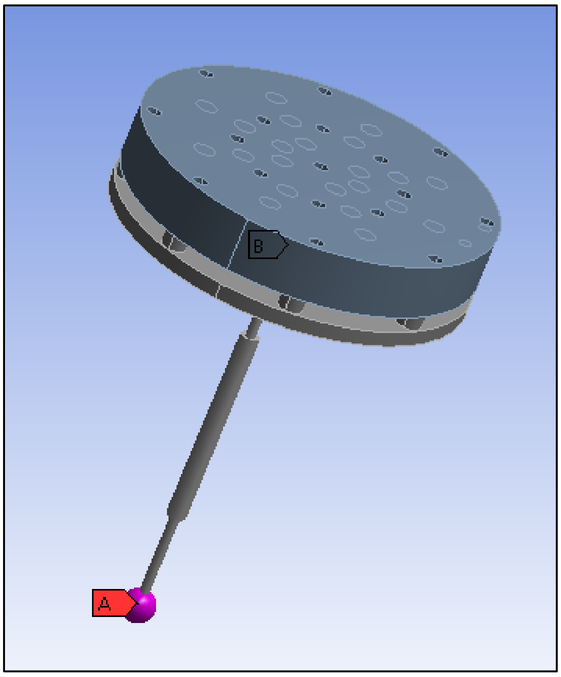

Figure 5.21. Shaker FE model with adapter plate

5.2.2 Full FE Model and Harmonic Response Analysis

After modeling the dynamics of the armature of the shaker using equivalent masses, a spring and a viscous damper, the vibration test fixture including two UUTs, is mounted on this model through the shaker adapter plate. All the connections between shaker, vibration test fixture parts and UUTs are made by bolts. Bolt connections are modeled according to pressure cone effect, referring to Richard G. Budynas (2014). Effective areas are defined and area pairs are bonded for each bolt connection. For instance, effective areas between shaker adapter plate and fixture bottom plate are seen in Figure 5.22.

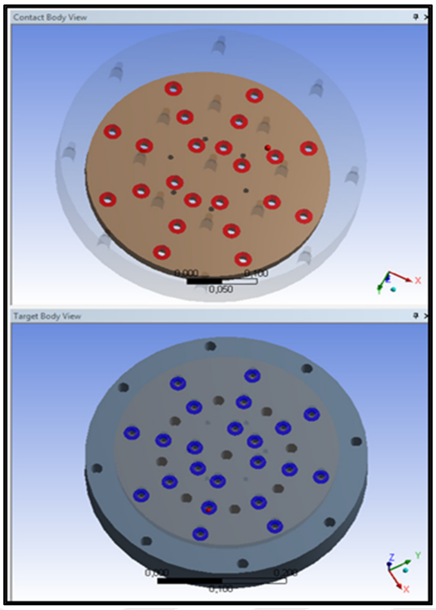

Figure 5.22. Bolt connection effective areas for the connection of adapter plate and fixture bottom plate

General aluminum alloy is selected in ANSYS as the material of the vibration test fixture parts and UUTs. Shaker adapter plate is also modeled as a flexible part in the FE model as it is seen in Figure 5.23.

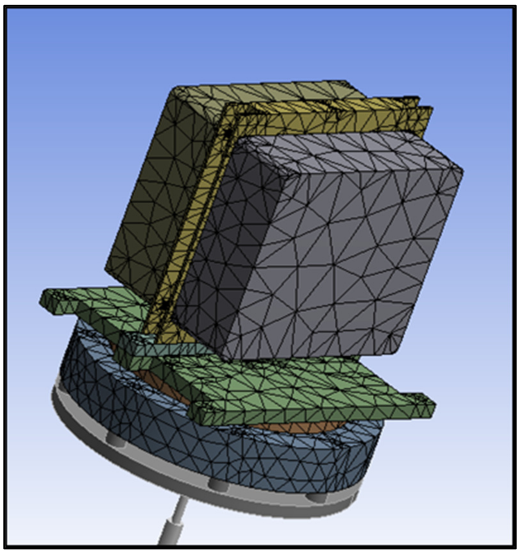

Figure 5.23. Full FE model with flexible adapter plate

Mode superposition harmonic analysis is performed by applying 1 N force at the lower mass of the armature where the force is created in real and it is also seen in Figure 5.24. 65 modes between 0 and 3170 Hz are used for the harmonic analysis between 4 Hz to 2000 Hz.

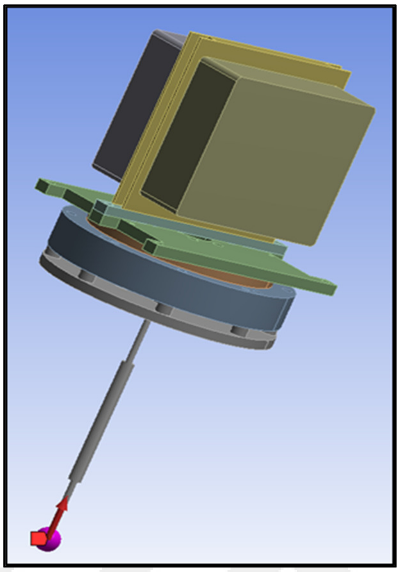

Figure 5.24. The force applied for harmonic analysis

In order to obtain transmissibility plot in FE model, Acceleration levels of two locations are found. These locations are seen in Figure 5.25 and Figure 5.26. They are the place where accelerometers were mounted for alternative test. Alternative test accelerometer locations are seen in Figure 5.27.

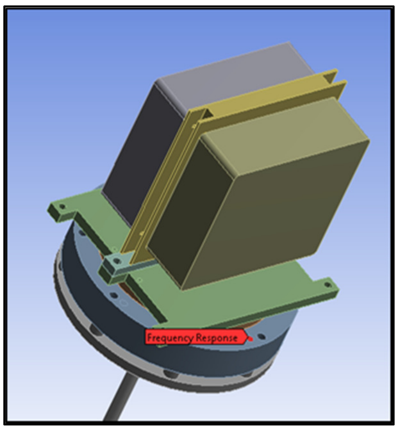

Figure 5.25. Control Accelerometer Location

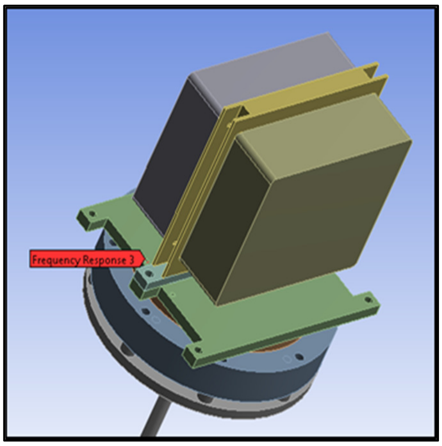

Figure 5.26. Monitor Accelerometer Location

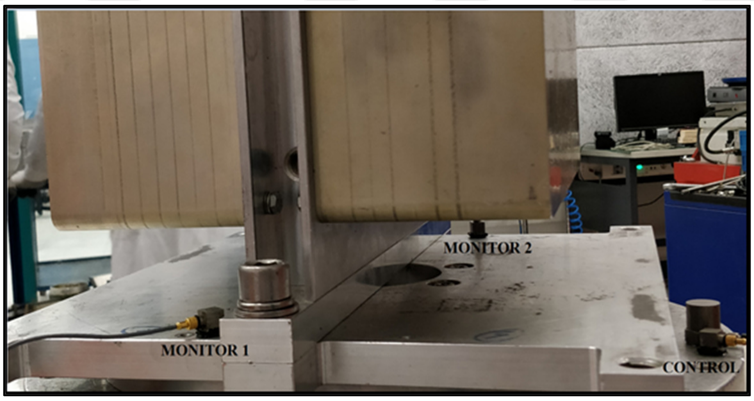

Figure 5.27. Real Transmissibility (Alternative) Test Configuration (Control and Monitor 1 is used)

The first transmissibility (monitor/control) comparison of the FE model (blue line) and test (black line) is seen in Figure 5.28 for 0.01 general damping ratio. It is seen that ANSYS model does not reflect dynamic behavior of the real system well and also transmissibility levels are much higher than test results.

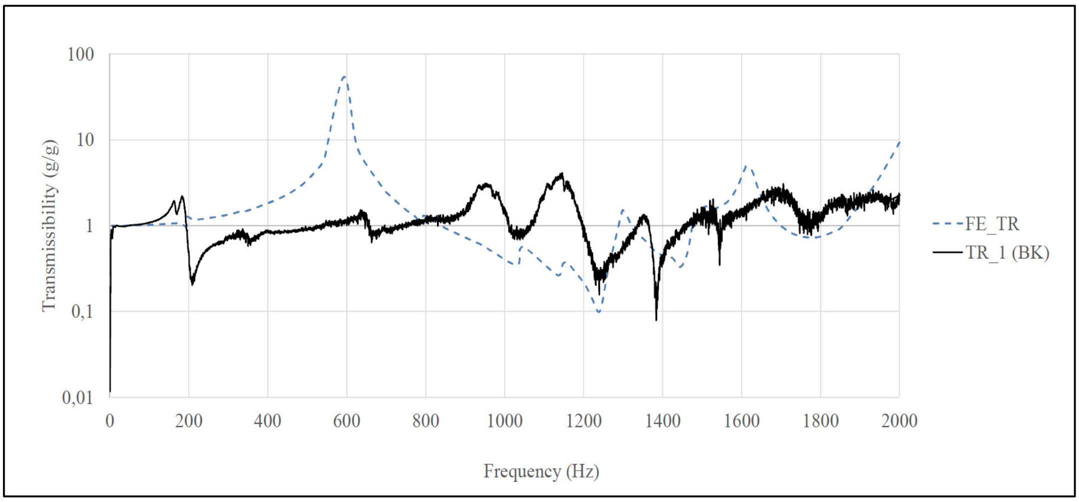

Figure 5.28. Real test & FE comparison (0.01 constant damping ratio)

During earlier study of vibration test fixture, a trial transmissibility test was performed without dummy UUTs as in Figure 5.29. It is seen in Figure 5.30 that TR test and ANSYS results are similar.

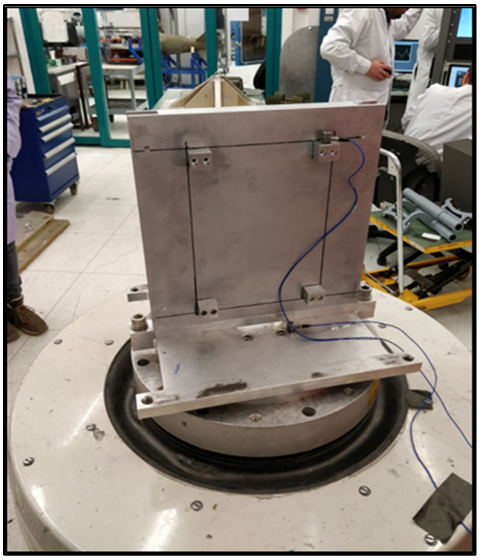

Figure 5.29. A trial TR test without dummy UUTs

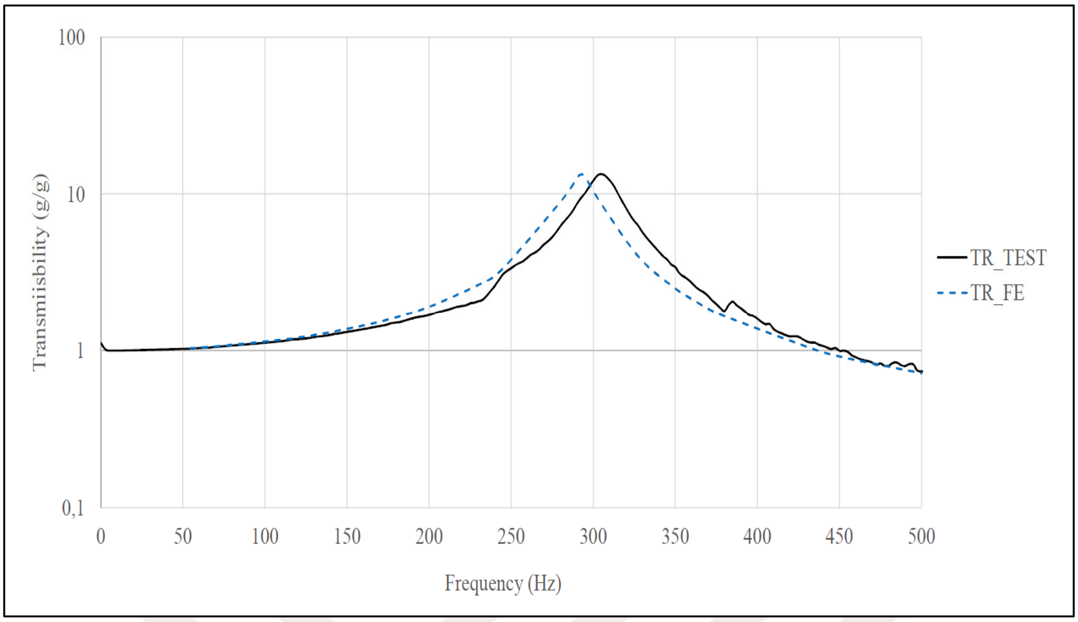

Figure 5.30. Trial TR Comparison Chart (Black Line: Real Test, Blue Line: ANSYS)

Similarity of TR lines without dummy UUTs implies that there can be a problem for UUT and vibration test fixture connection. As it is mentioned earlier, pressure cone effect method is used for all bolt connections and effective areas for dummy and fixture connection interface is seen in Figure 5.31. However, bolts for mounting UUTs are exposed to shear stress because motion (test) direction is perpendicular to bolts' longitudinal axes. In order to model UUT & vibration test fixture interface more accurately, bolts are modeled as solid parts and inserted into assembly. Each bolt is fixed to vibration test fixture via the area under cap as it is seen in Figure 5.32. Cylindrical surfaces of the bolts are fixed to cylindrical surfaces of UUT connection holes as in Figure 5.33. Thus, UUTs are connected to vibration test fixture in a more realistic manner. New transmissibility comparison plot is seen in Figure 5.34.

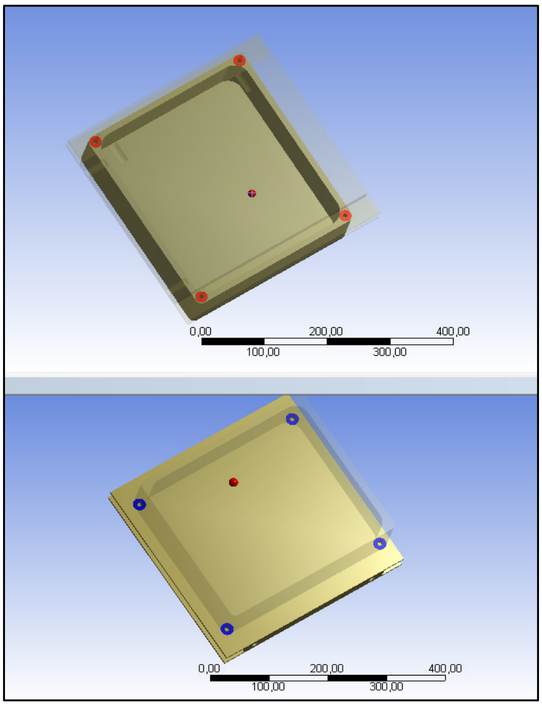

Figure 5.31. Initial connection of UUTs by pressure cone method

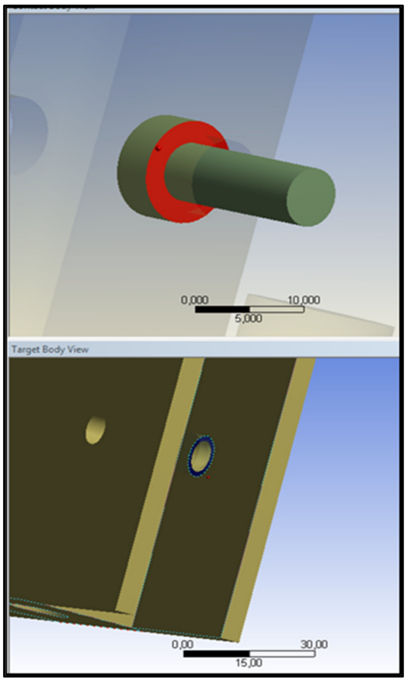

Figure 5.32. Bolt & fixture connection areas

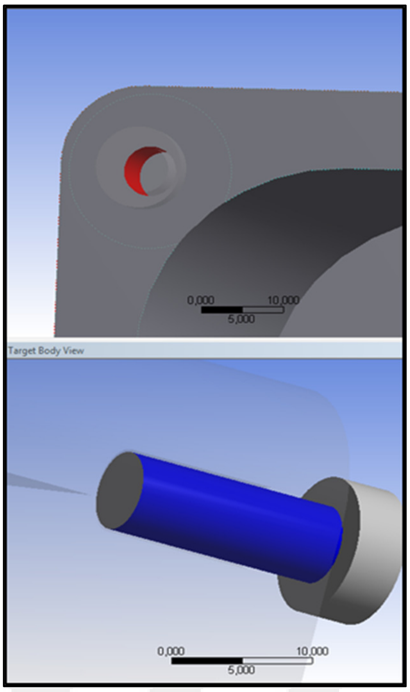

Figure 5.33. Bolt & dummy UUT connection areas

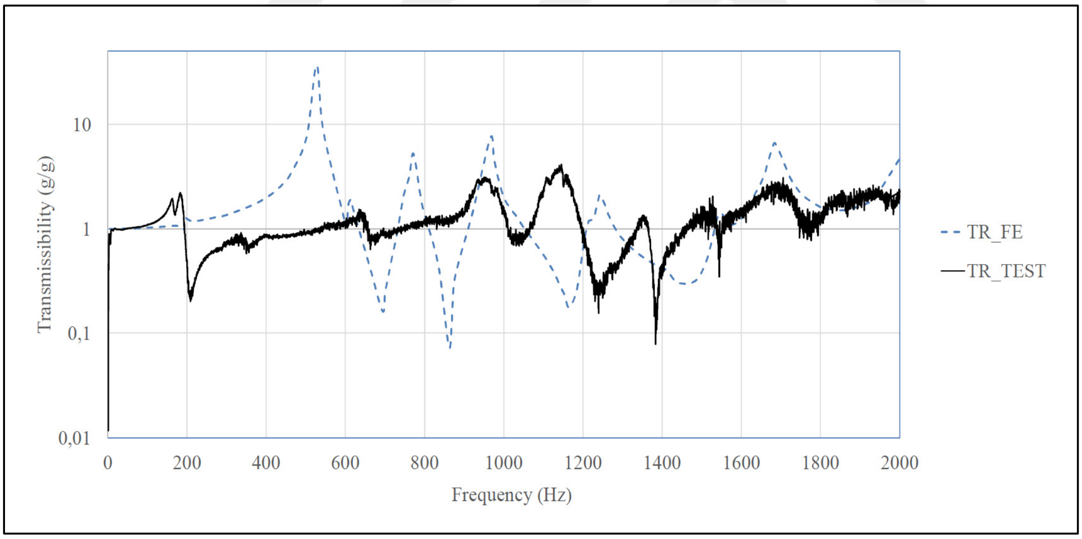

Figure 5.34. Real Test & FE Comparison with Bolted UUT (0.01 Constant Damping Ratio)

Model with bolted UUTs has closer TR levels than initial model as seen in Figure 5.34. However, divergence of TR around 600 Hz still exists and the frequency is lower this time in ANSYS results as it is compared to real test results. Connection areas of the monitor accelerometer mounting plate are increased in order to match the resonance frequency around 600 Hz and increase rigidity. Connection areas are increased from 50 mm to 65 mm as it is seen in Figure 5.35.

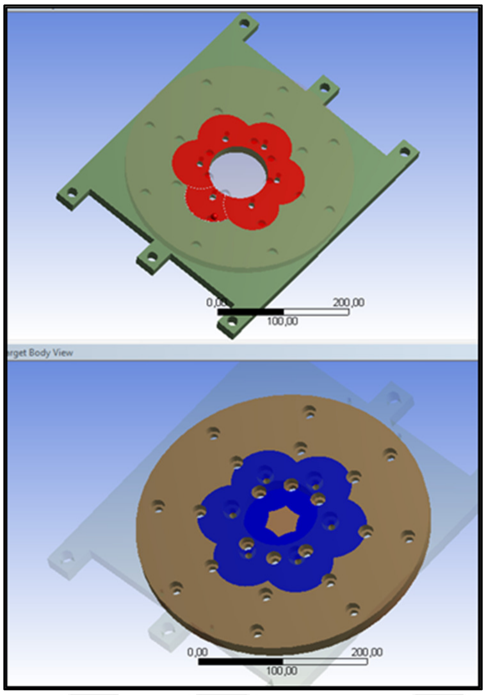

Figure 5.35. Increased bolt area for UUT (65 mm)

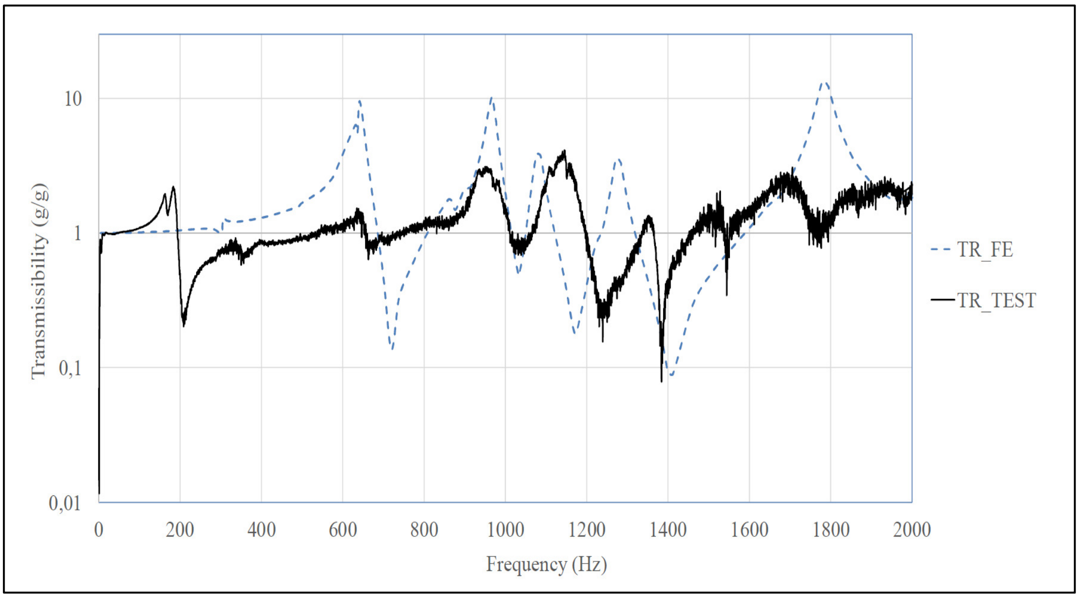

Figure 5.36. Real Test & FE Comparison with Bolted UUT and 65 mm Base Mount for Each Bolt (0.01 Constant Damping Ratio)

It is seen in Figure 5.36 that the problem around 600 Hz is fixed. In order to fit higher modes more closely, connection areas of fixture parts should be increased. Firstly, mounting surfaces of the highlighted parts in Figure 5.37 are aimed to be increased. Initial connection surfaces are seen in Figure 5.38 and additional connection surfaces are seen in Figure 5.39.

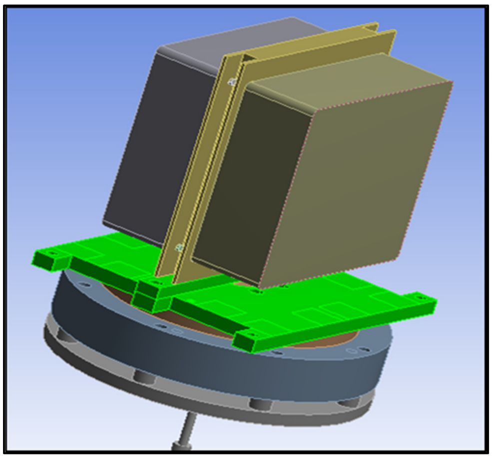

Figure 5.37. Highlighted parts (Pair 1)

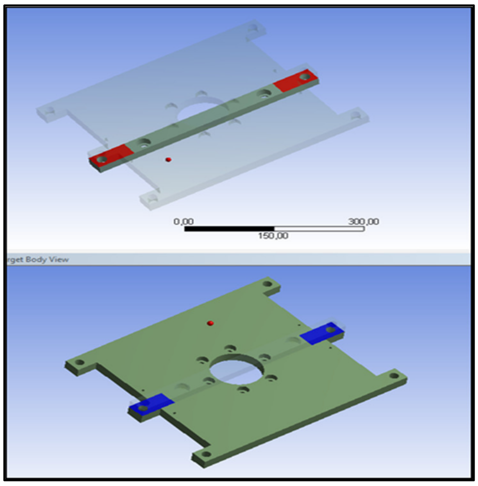

Figure 5.38. Pair 1, Initial connection surfaces

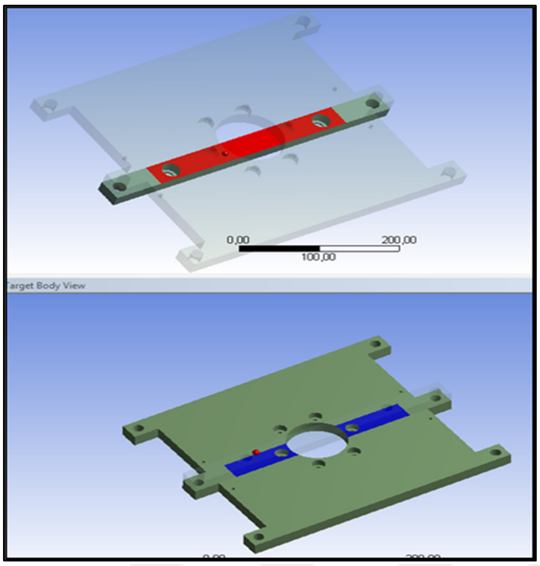

Figure 5.39. Pair 1, Added connection surfaces

Secondly, mounting surfaces of the highlighted parts in Figure 5.40 are also increased. Initial connection surfaces for pair 2 are seen in Figure 5.41 and additional connection surfaces are seen in Figure 5.42.

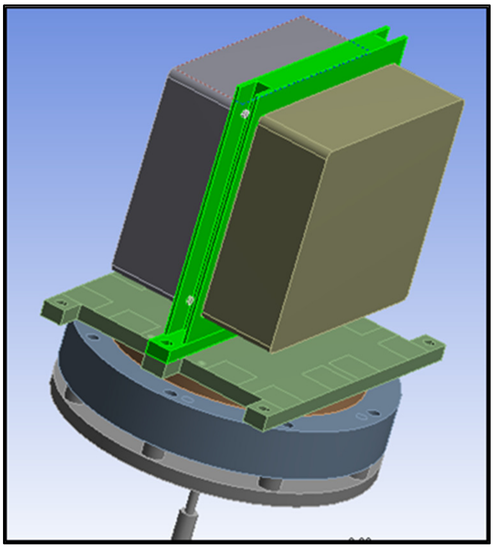

Figure 5.40. Highlighted parts (Pair 2)

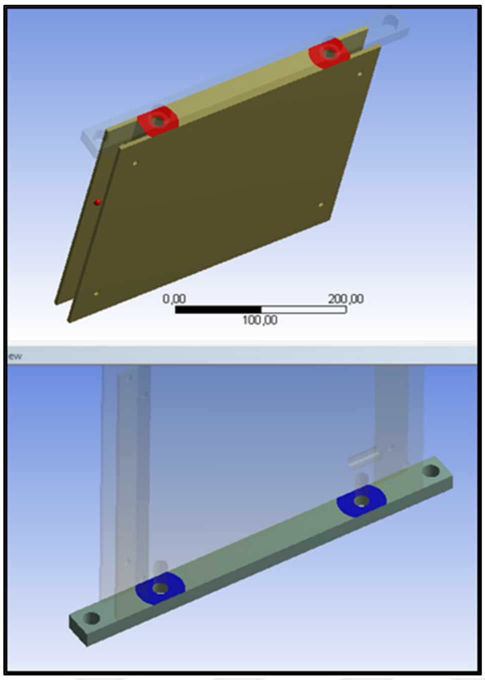

Figure 5.41. Pair 2, Initial connection surfaces

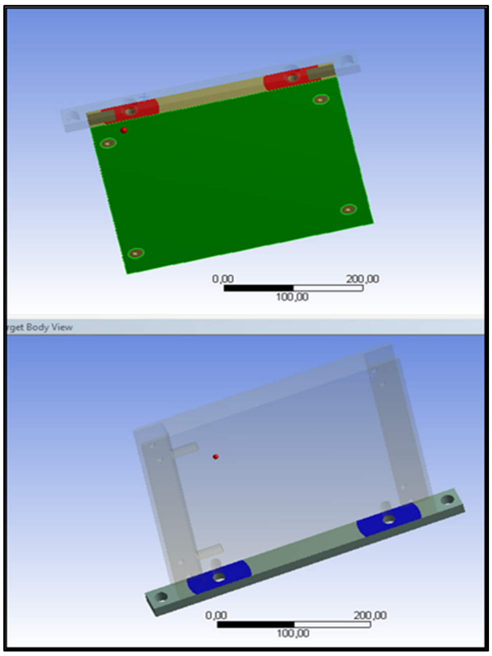

Figure 5.42. Pair 2, Increased connection surfaces

After some trials, 0.02 constant damping ratio is used in order to fit FE transmissibility plot and alternative test transmissibility plot more closely. Final transmissibility (monitor/control) comparison of the final FE model (blue line) and test (black line) is seen in Figure 5.43.

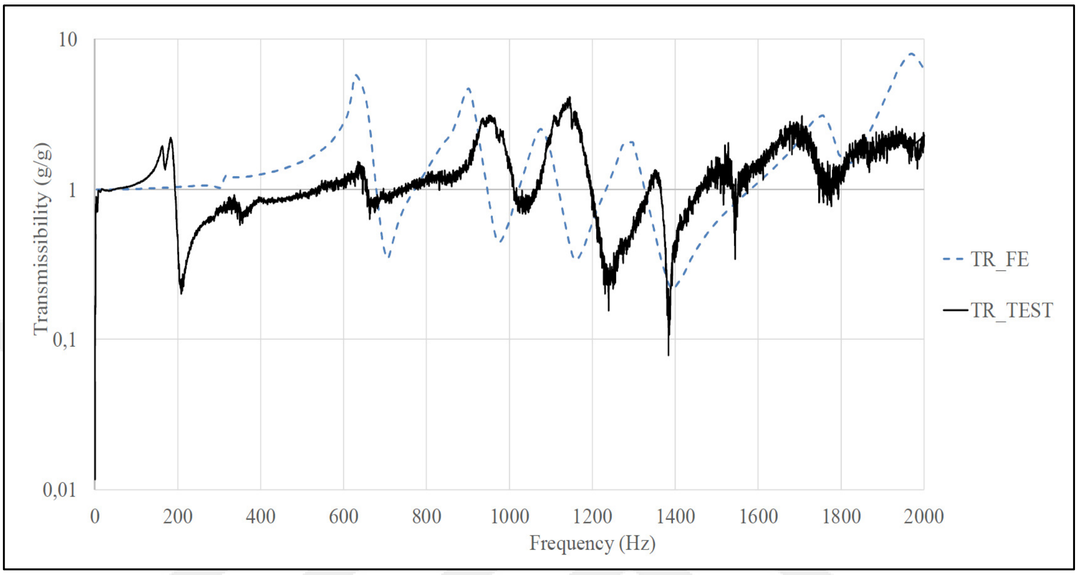

Figure 5.43. Transmissibility plot (final FE & real test comparison)

Figure 5.43 implies that the FE model reflects the dynamic characteristics of the real model except for the modes around 200 Hz which are not seen in FE transmissibility plot. It is thought that, these mode(s) refer to rotational modes of the armature with its guides and FE model does not contain the effect of rotational modes. As it was mentioned before, the vibration test fixture is intended to use for three test directions. Due to its design limitations, center of gravity could not be centered for Z direction test and unaligned COG of the vibration test fixture & UUT assembly creates moments during real tests which excite the rotational modes.

Two hammer tests were performed in order to inspect the existence of rotational modes at lower frequencies. The soft tip of the hammer was used to excite lower frequencies in a better way. During the first test, the hammer excited the system from the location where control accelerometer was located for transmissibility test.

Secondly, the hammer excited the system from the cylindrical surface of the adapter plate. Hammer hit points are showed as the cross marks in Figure 5.44.

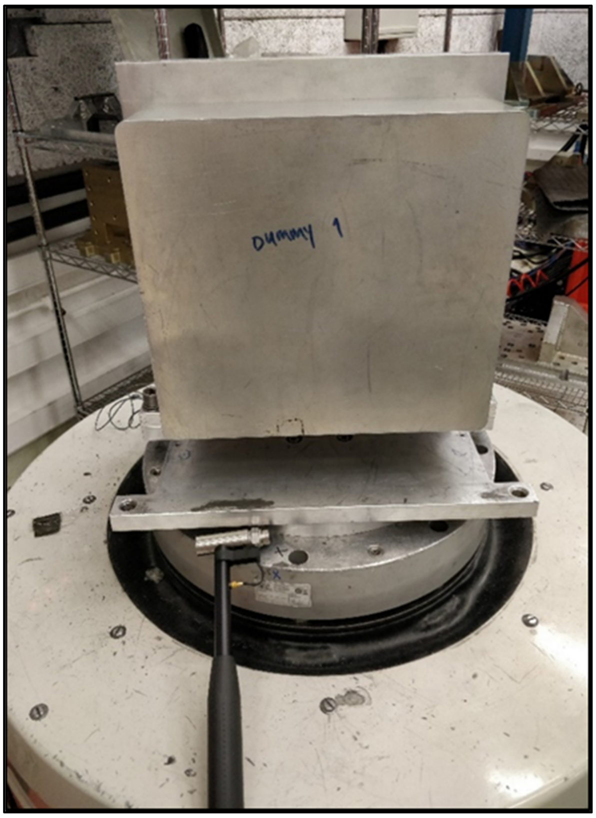

Figure 5.44. Hammer test setup and hammer hit locations

Although the FRF units are different in Figure 5.45 (g/g and ms^{-2}/N), resonant behavior at interested frequency region can be seen clearly. These modes are considered to be rotational modes of the armature & linear guide assembly and they can be taken as out of consideration because during the original aborted test, vibration profile follows the target profile around those frequencies.

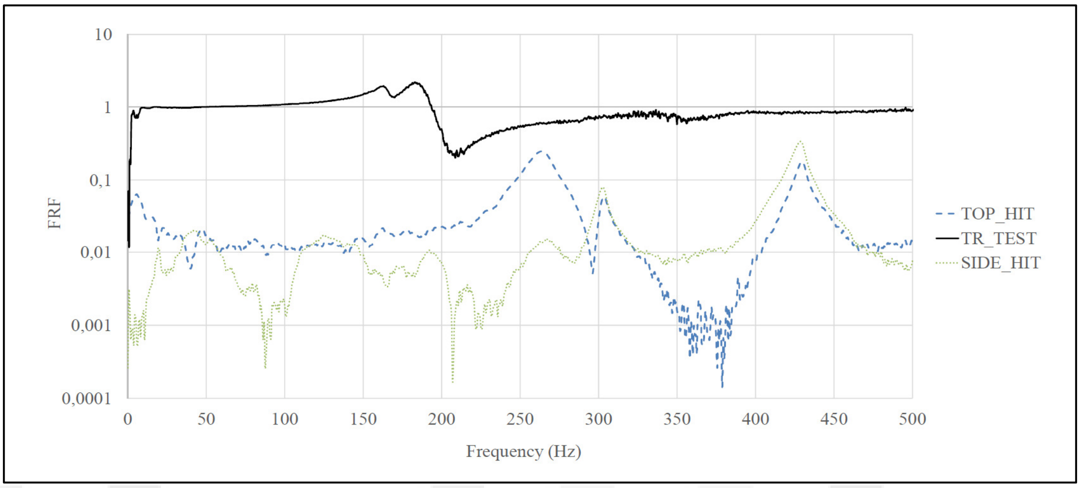

Figure 5.45. Rotational modes (hammer tests and transmissibility test)

5.2.3 Mesh Convergence Analysis

This analysis is performed to check that resonant frequencies of the ANSYS model is insensitive to mesh size. When the optimized mesh size is obtained, it is used for all other FE analyses. Mode seven is taken as the target mode and after fifth iteration modal frequency is insensitive to mesh refinement as it is seen in Figure 5.46. On the other hand, fine mesh causes time consuming analyses and sometimes hardware is not enough for performing analysis. Therefore 10% tolerance with respect to converged frequency is taken and a solvable mesh size is defined as in the last row of Table 5.3.

Table 5.3 Total Element Number and Related 7th Modal Frequency

7th Modal Frequency (Hz)	*Total Mesh Element Number*
641.35	87443
642.06	71107
647.59	59858
663.63	47327
671.86	39431
692.03	29113

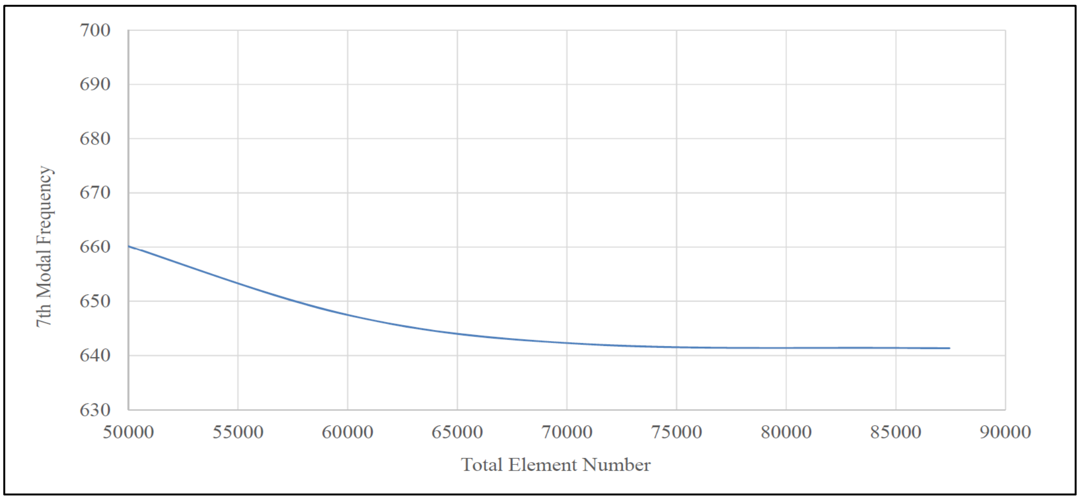

Figure 5.46. Convergence Plot for the 7th Modal Frequency

5.2.4 TVA Treatments for the Problematic Regions

As it was mentioned earlier, the first target frequency is 935 Hz where the highest peak occurs for the aborted random vibration test. Firstly, the related mode shape must be found from FE model which can be seen in Figure 5.47. The resonant frequency is around 921 Hz for the FE model. It is seen that this mode is the local mode of the plate where control accelerometers are mounted in the real test.

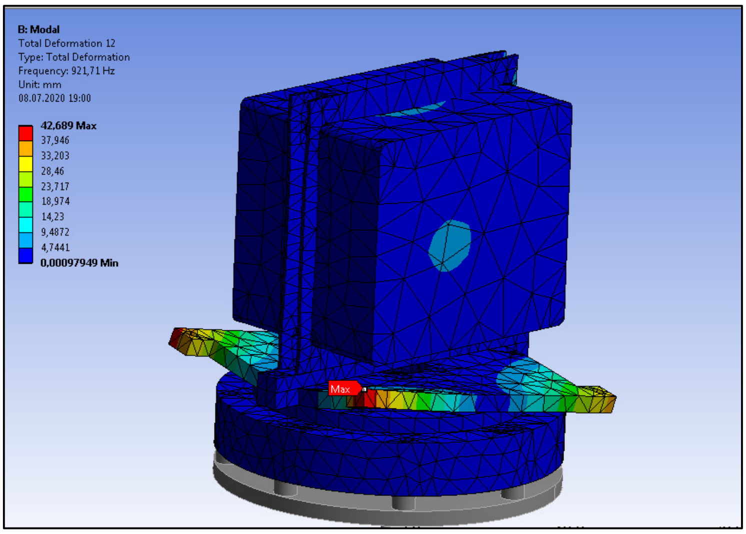

Figure 5.47. Related mode shape in FE model (921 Hz)

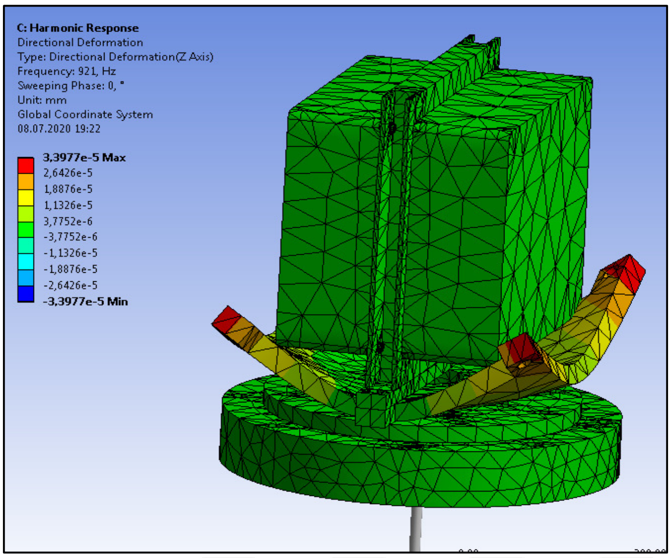

Figure 5.48. Z axis deformation in harmonic response analysis (921 Hz)

In order to dissipate the vibration energy for this mode, damping should be increased by a proper structural modification technique. Four identical tuned vibration absorbers are intended to mount near the maximum deflected zones of the accelerometers mounting plate as it is seen in Figure 5.48.

Viscoelastic materials are highly damped materials which can be used for producing TVAs. The damping is due to internal material friction which is called hysteretic or structural damping. However, dynamic properties of a viscoelastic material is highly dependent on working frequency and temperature and nomograms are used to find these interrelated parameters. For a hysterically damped single degree of freedom lumped mass model, equivalent viscous damping coefficient can be found by comparing energy losses in one vibration cycle. It is found as in Equation (5.6).

$$c_{eq} = h / \omega \tag{5.6}$$

Where c_{eq} is the equivalent viscous damping coefficient, h is the hysteretic (structural) damping coefficient and ω is the excitation frequency. Equivalent damping ratio can be written for the equivalent viscously damped system as in Equation (5.7).

$$\zeta_{eq} = c_{eq} \,/\, c_{critical} = h / (2m\ \omega_n \omega) \tag{5.7}$$

And natural frequency can be written as in Equation (5.8).

$$\omega_n = (k / m)^{1/2} \tag{5.8}$$

where $c_{critical}$ is the critical damping coefficient, m is the mass, ω_n is the natural frequency and k is the stiffness coefficient. When ω is equal to ω_n, modal damping ratio can be found in Equation (5.9).

$$\zeta_{eq} = h / (2k) \tag{5.9}$$

By rearranging Equation (5.9), Equation (5.10) is formed.

$$2\zeta_{eq} = h / k \tag{5.10}$$

The h / k term in Equation (5.10) and Equation (5.11) is called as the loss factor (η) which indicates the ratio of lost energy and stored energy.

$$\eta = 2\zeta_{eq} = h / k \tag{5.11}$$

On the other hand, complex modulus of elasticity concept is used for materials in order to indicate stored and lost energy and it is formulated in Equation (5.12).

$$E = E^{I} + iE^{II} \tag{5.12}$$

where E is the complex modulus of elasticity, E^{I} is the storage modulus and E^{II} is the loss modulus and i is the complex number. Loss factor can also be stated as the ratio of loss modulus of elasticity and storage modulus of elasticity as in Equation (5.13).

$$\eta = E^{II} \,/\, E^{I} \tag{5.13}$$

Complex modulus of elasticity and loss factor can be found with respect to working frequency and temperature by using the nomogram of the selected viscoelastic material.

For this study, a viscoelastic material is selected in the market which has a high damping capacity around 935 Hz. 3M-467 MP is chosen which is a double sided adhesive transfer band with a thickness of 0.05 mm. Dynamic properties of 3M-467 MP are found by using the nomogram taken from A.D. Nashif, David I.G. Jones (1985). In order to use the nomogram, a horizontal line is drawn from the desired working frequency. The point where the horizontal line intersects with the constant working temperature line must be found and room temperature is taken as the working temperature for this application. A vertical line should be drawn from the marked point, points where the vertical line crosses the complex modulus of elasticity curve and the loss factor curve, indicate the values of material properties. Poission ratio do not change much by temperature and frequency and an average value of 0.35 is used as the material property.

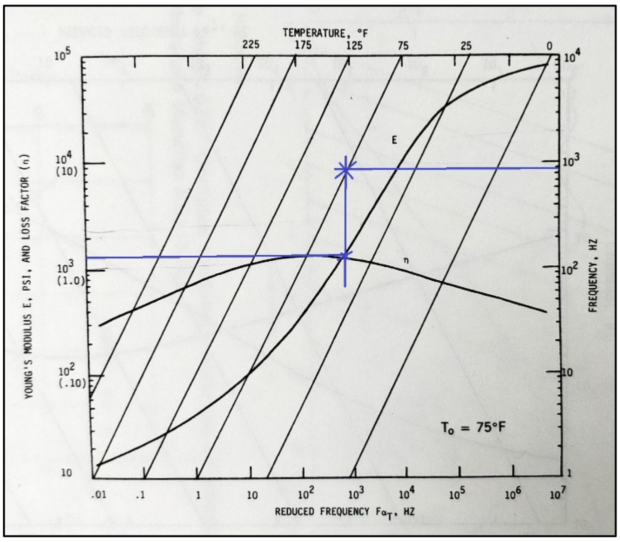

Figure 5.49. 3M-467 MP nomogram (A.D. Nashif, David I.G. Jones, 1985)

Complex modulus and loss factor are found from Figure 5.49 and tabulated in Table 5.4.

Table 5.4 Mechanical properties of 3M-467 MP around 935 Hz

Complex Elastic Modulus (Pa)	*Loss Factor*	*Storage Modulus (Pa)*	*Loss Modulus (Pa)*	*Density (kg/m^3) *Taken from the product catalogue*
8963187.464	1.3	5464940.084	710442.60	1012

In Figure 5.50, the TVA is modeled by mass, spring and a damping element separately in another FE model, which is tuned to 921 Hz with 0.65 damping ratio as the half of loss factor which is stated in Equation (5.11). Mass of each TVA is selected by trial and error method and 0.8 kg is seen to be effective by checking the result on TR comparison plot.

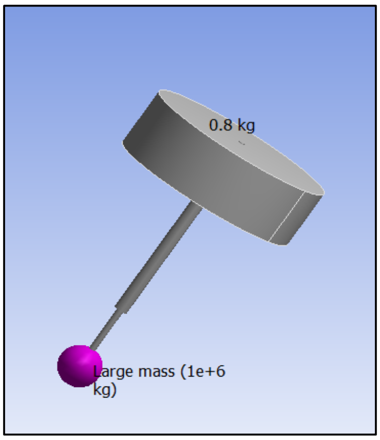

Figure 5.50. Stand alone TVA model

Modal frequencies of the stand alone TVA is seen in Figure 5.51. The first mode of the stand alone TVA model is rigid body mode which is out of consideration and the second mode is the desired mode which has the desired resonant frequency.

	Mode	☑ Damped Frequency [Hz]	☐ Stability [Hz]	☐ Modal Damping Ratio
1	1,	1,3416e-008	0,	0,
2	2,	921,18	-795,78	0,65372

Figure 5.51. Stand alone TVA modes

In Figure 5.52, related spring and damping elements are seen. Stiffness and damping coefficients are found as 46800 N/mm and 8 N.s/mm respectively by trial and error method in order to meet damping ratio and resonant frequency requirements.

Longitudinal Stiffness	46800 N/mm
Longitudinal Damping	8, N·s/mm

Figure 5.52. Stand alone TVA spring and damping coefficients

After tuning stand alone TVA model, TVAs are inserted into the full FE model as in Figure 5.53. It is seen that the peak around 921 Hz is eliminated in transmissibility plot in Figure 5.54 after the first TVA treatment.

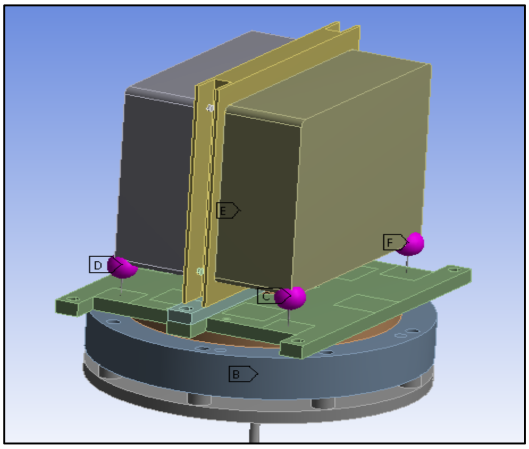

Figure 5.53. TVA added FE model (1st TVA Treatment)

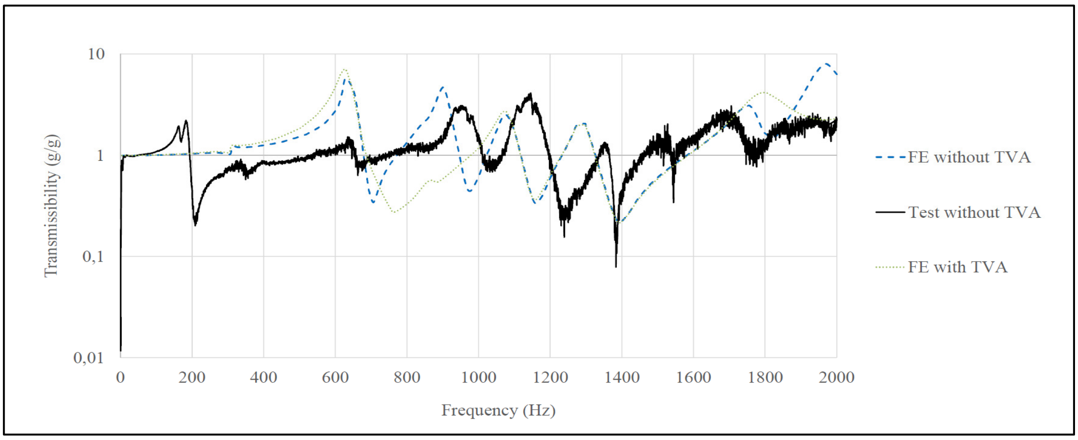

Figure 5.54. Transmissibility Comparison Chart After First TVA Treatment

As a result of the elimination of the peak around 921 Hz in Figure 5.54, it is expected that resonance problem around 935 Hz in random vibration test is going to be fixed by the first TVA treatment.

In order to insert TVAs into the real test setup, TVAs must be designed and then they must be manufactured properly. Firstly, CAD model of the TVA is created with an initial thickness of 3M 467 MP which is seen in Figure 5.55. Followingly, CAD model is inserted in FEA program. Material properties of 3M 467 MP are inserted into the FEA program as in Figure 5.56. In addition, loss factor is defined for 3M-467 MP by using MP,DMPS,1,1.3 command in ANSYS command manager.

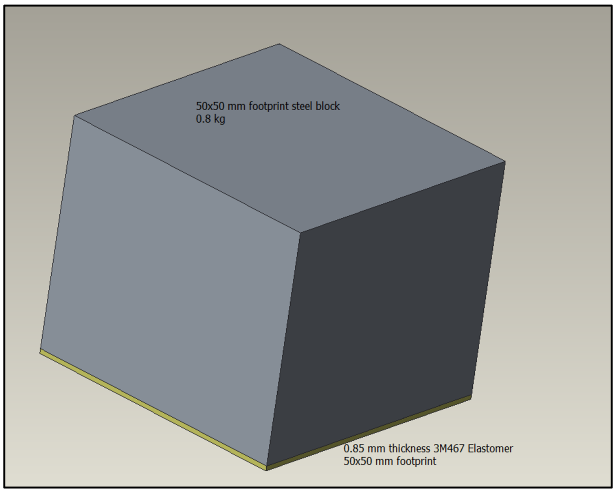

Figure 5.55. CAD model of the TVA

Properties of Outline Row 3: 3m467

	A	B	C
1	Property	Value	Unit
2	Material Field Variables	Table	
3	Density	1012	kg m^-3
4	Isotropic Secant Coefficient of Thermal Expansion		
5	Coefficient of Thermal Expansion	1,2E-05	C^-1
6	Isotropic Elasticity		
7	Derive from	Young's Modulus and...	
8	Young's Modulus	5,4649E+06	Pa
9	Poisson's Ratio	0,35	

Figure 5.56. Material properties of 3M-467 MP in ANSYS

Required thickness of the 3M 467 MP is found as 0.85 mm after some iterations by tuning the longitudinal modal frequency of TVA FE model to 935 Hz which is seen in Figure 5.57. This means that lamination of 17 layers of 3M-467 MP are required for each TVA.

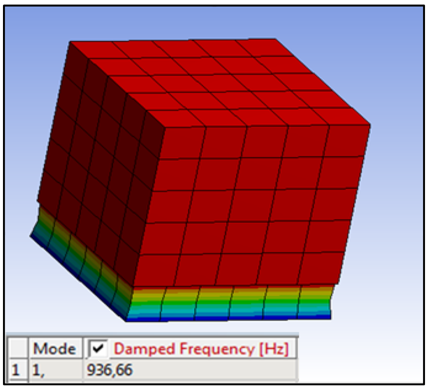

Figure 5.57. FE model of the first TVA

In order to produce TVAs, a stainless steel block mass is intended to use as the mass of the TVA. Lamination process is performed layer by layer with special care in order to prevent sentenced bubbles between layers which distort dynamic performance of the TVA. A TVA which is ready for mounting on the vibration test fixture is seen in Figure 5.58.

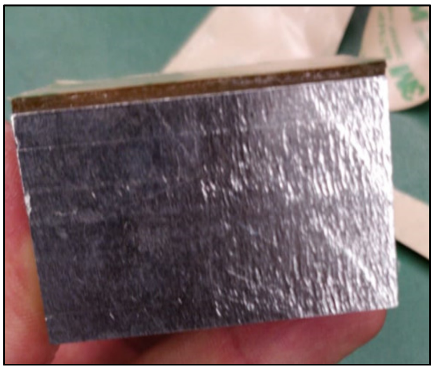

Figure 5.58. Laminated TVA

As it was mentioned before, four TVAs are tuned to target frequency of the aborted test (935 Hz) and mounted on the same locations as in the FE model which is seen in Figure 5.59.

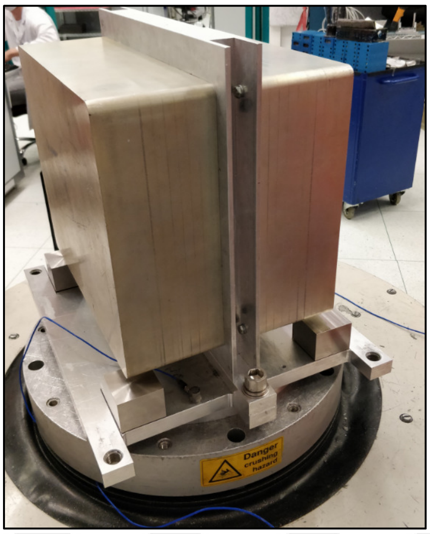

Figure 5.59. Full test setup with the first TVA treatment

After mounting TVAs, original random vibration test is performed again and it is seen the problematic region around 900 Hz is fixed as in Figure 5.60. Nevertheless test was aborted because of the problems in the higher frequencies.

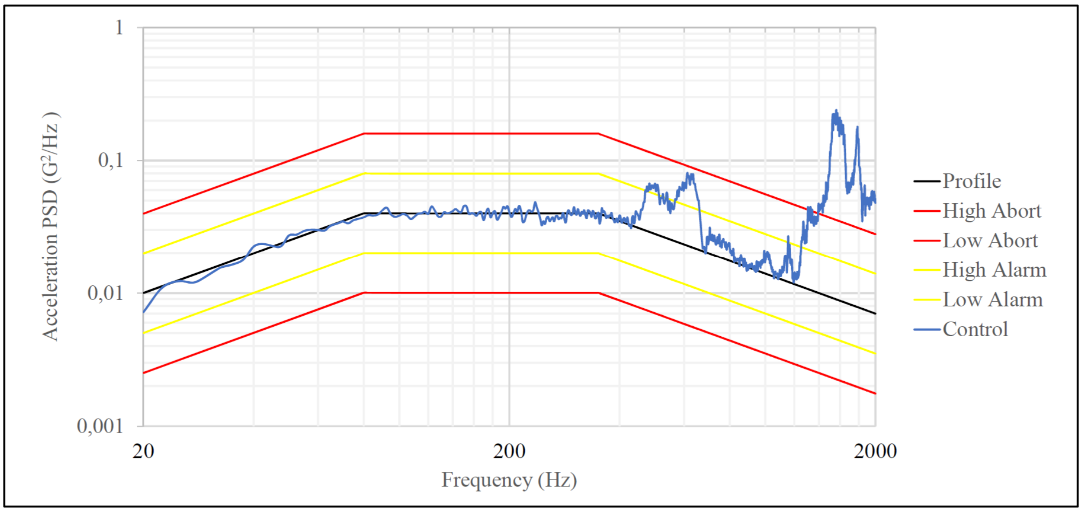

Figure 5.60. New aborted test with the first TVA treatment

In Figure 5.61, another transmissibility test is performed to check how the transmissibility has changed:

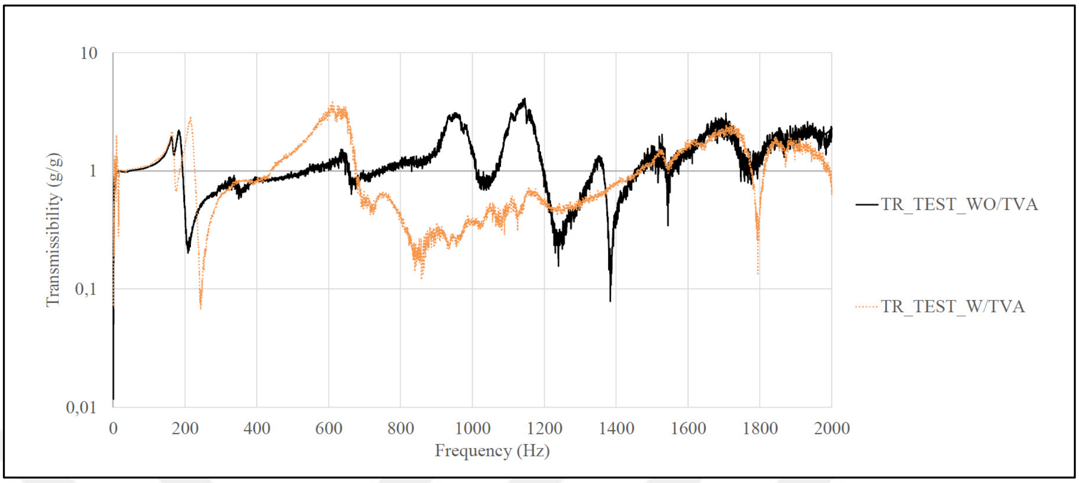

Figure 5.61. Real Transmissibility Tests Comparison Chart (without TVA, with 1st TVA treatment)

If we check the new aborted test in Figure 5.60, the highest peak is around 1780 Hz which is our next target frequency. The related mode shape can be found by FE model as in Figure 5.62.

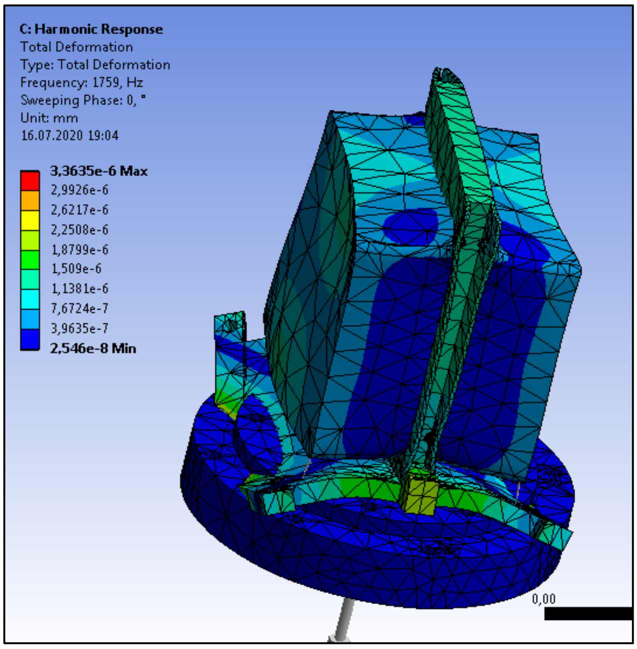

Figure 5.62. Total Deformation in Harmonic Response Analysis (1759 Hz)

In order to absorb the energy at this mode, it is aimed to locate the TVA on top of the UUT mounting plate which has a high level of motion with respect to other TVA mountable locations. A 7.5 kg block mass is used with the same viscoelastic material which has a loss factor around 1.0 for 1759 Hz region. The second TVA is tuned to 1759 Hz and whole FE model with the second TVA treatment is seen in Figure 5.63.

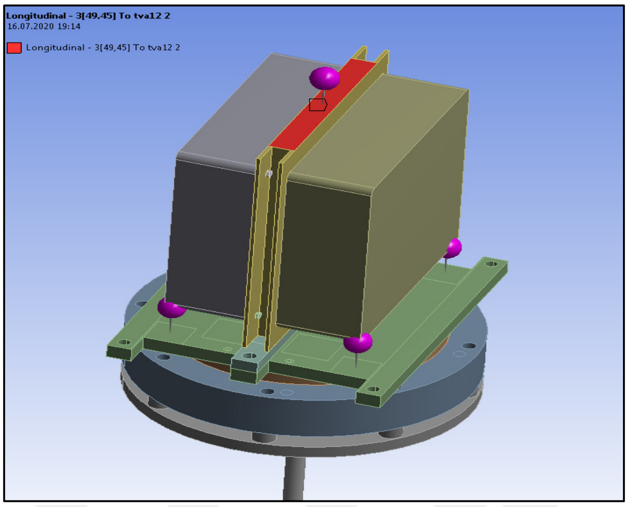

Figure 5.63. FE model with the second TVA treatment

All the TVA treatment processes are the same as in the first TVA treatment. After the second TVA treatment, FE modified transmissibility plot in Figure 5.64 shows that the peak around 1759 Hz is eliminated.

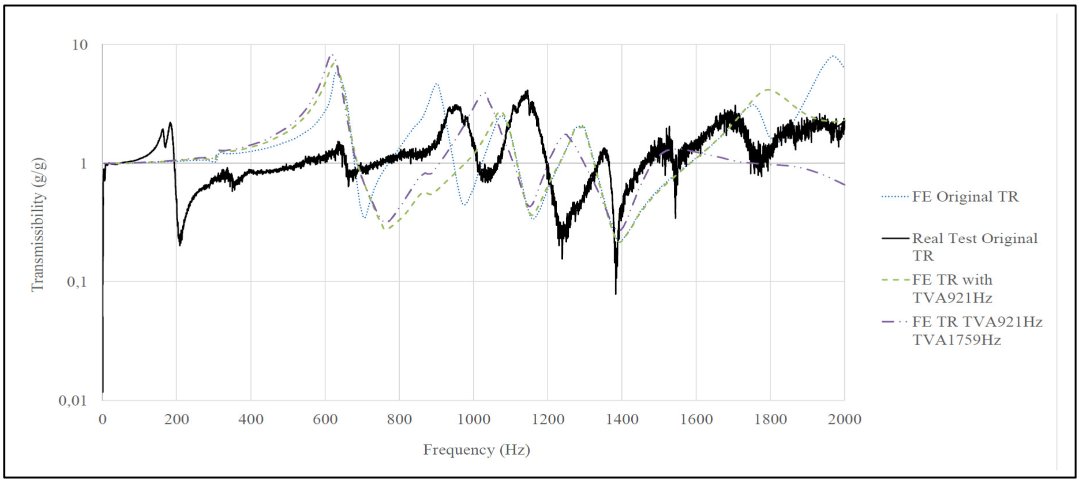

Figure 5.64. Transmissibility comparison chart after the second TVA treatment

In order to test the effect of the second TVA, a physical TVA is designed and constructed which is tuned to 1780 Hz that is the actual target frequency and mounted on the same place as in the FE model. FE model of the second TVA with a 7.5 kg steel block mass and 3 layers of 3M-467 MP is seen in Figure 5.65.

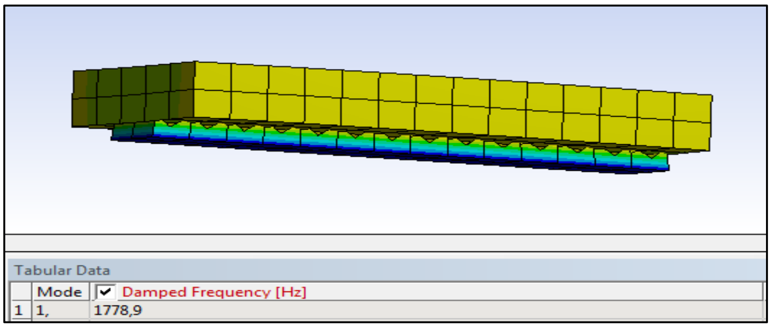

Figure 5.65. FE model of the second TVA

Full test setup after the second TVA treatment is seen in Figure 5.66.

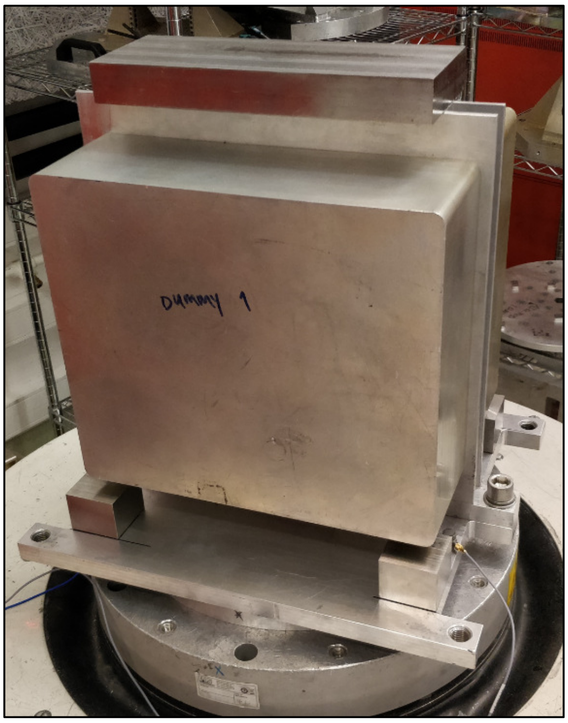

Figure 5.66. Full test setup after the second TVA treatment

Actual random vibration test is performed again and it is seen in Figure 5.67 that the test is not aborted by the high line error which is the cause of previous tests to abort. All the vibration levels of the test frequency range are within the test tolerance band. It is also realized that the shaker controller is able to control the resonance behavior around 600 Hz without any special TVA treatment for that region. After two TVA treatments, severe resonant regions which cause test to abort are eliminated. This gives ability to the controller to adjust drive signal without reaching any high line abort.

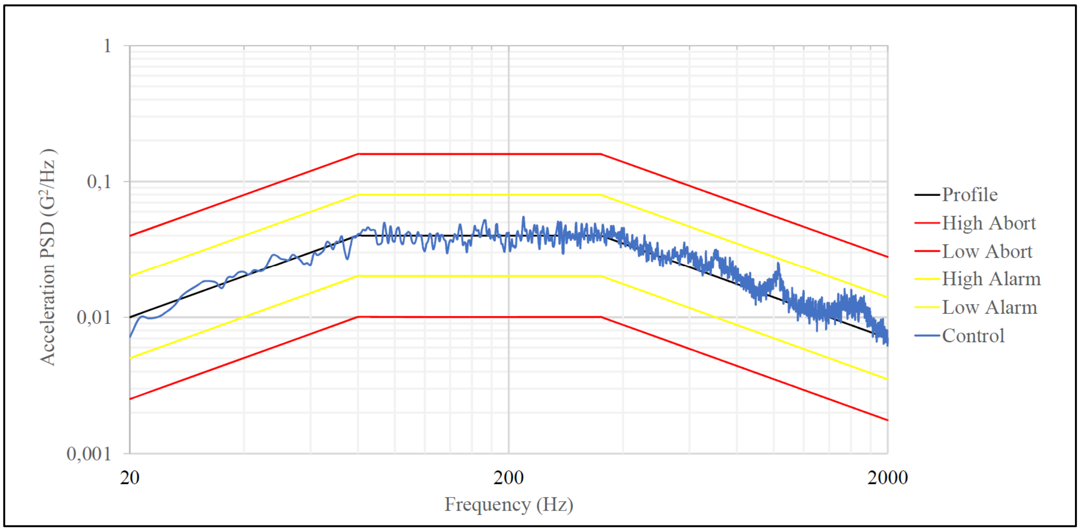

Figure 5.67. Successful random vibration test after second TVA treatment

5.2.5 Different TVA Combinations for Checking TVA Performances

In the previous section, two TVA combinations are used to perform the random vibration test. The first combination consists of TVAs which are tuned to 935 Hz. When the random vibration test is run again with the first TVA combination, it is seen that the real random vibration test profile follows the desired profile around 900 Hz region but the real random vibration test is out of tolerance around 1780 Hz. Then, it is aimed to create the second TVA combination by adding the TVA for 1780

Hz. It is seen that random vibration test is performed successfully with the second TVA combination.

In order to see how effective mass of a TVA effect the test behavior, the third TVA combination is created. This combination consists of the same TVAs for 935 Hz and three TVAs for 1780 Hz which have 1 kg effective mass seperately as in Figure 5.68.

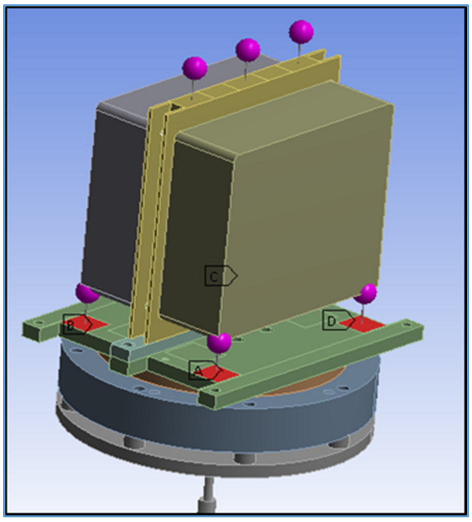

Figure 5.68. FE model with the third TVA combination

It is seen from Figure 5.69 that the peak around 1780 Hz can not be fully eliminated by using the third TVA combination.

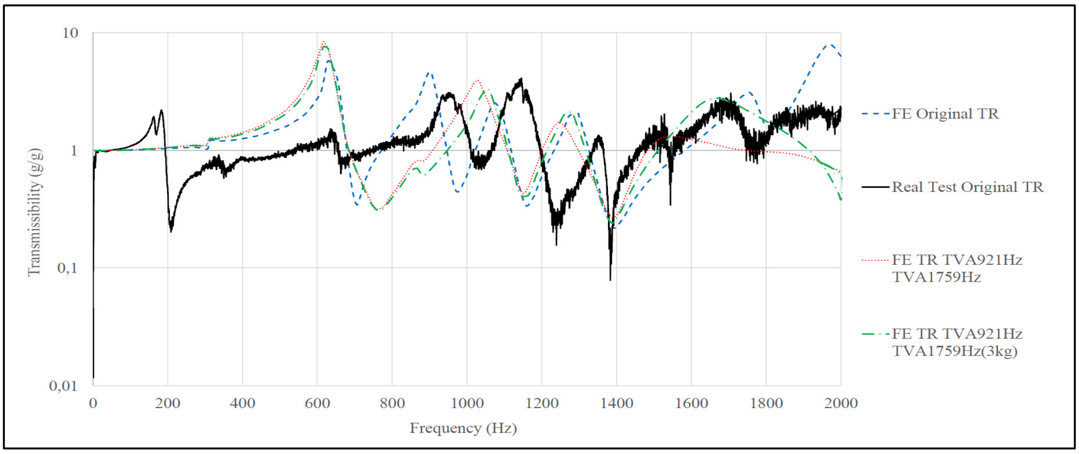

Figure 5.69. Transmissibility comparison plot for the FE model with the third TVA Combination

Three TVAs are physically produced and mounted on the vibration test fixture as it is seen in Figure 5.70. Random vibration test is perfomed again with the third TVA combination and it is seen in Figure 5.71 that the desired random vibration profile can not be achieved at high frequency region. It means that total effective mass of 3 kg is not adequate to absorb unwanted energy around 1780 Hz.

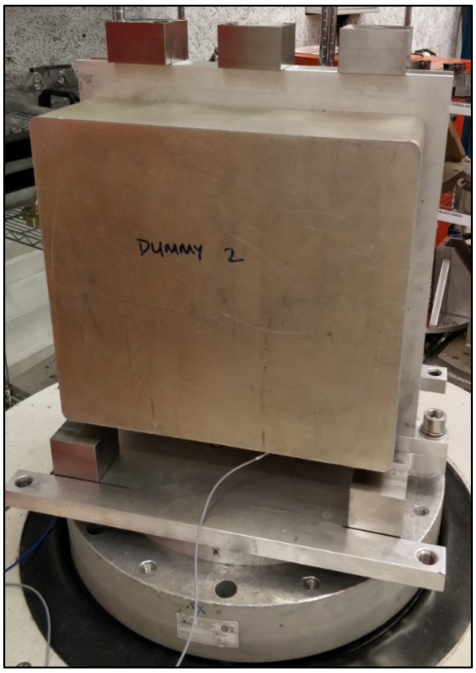

Figure 5.70. Test setup with the third TVA combination

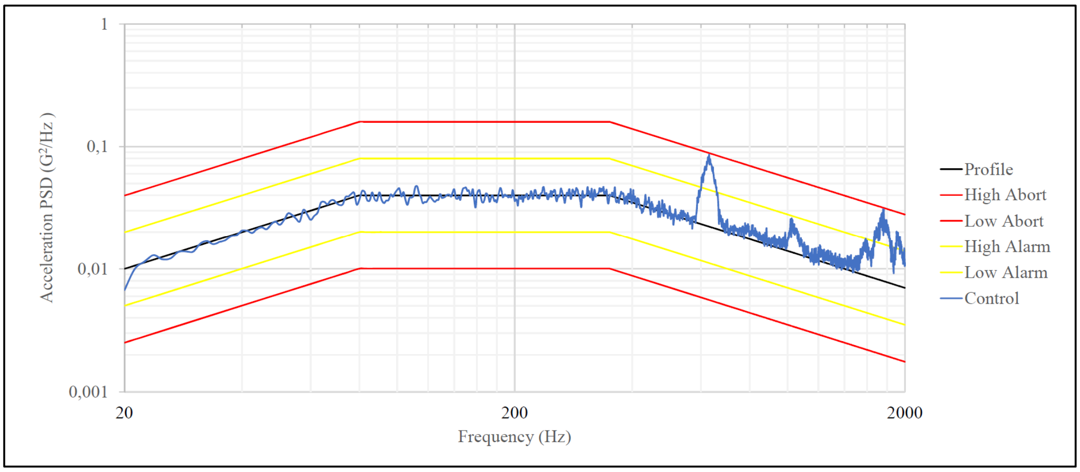

Figure 5.71. Random vibration test result with the third TVA combination

The fourth TVA combination is created by extracting all TVAs for 935 Hz from the third combination.

Transmissibility comparison plot is seen in Figure 5.72 for the fourth TVA combination. It implies that the peak around 935 Hz remains in the system. It is expected to have severe resonant behaviour around 900 Hz again and random vibration test can be aborted as in the inital case due to high resonant behavior.

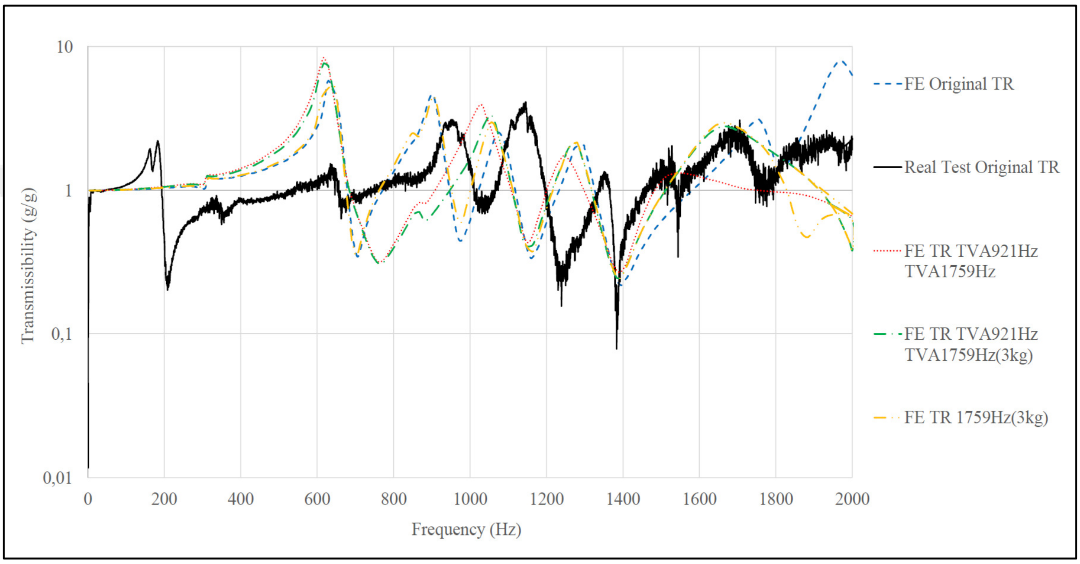

Figure 5.72. Transmissibility comparison plot for the FE Model with the fourth TVA combination

Before performing random vibration test again, TVAs for 935 Hz are simply unmounted by applying torsional load on the TVA masses. Then, the fourth TVA combination is created as in Figure 5.73.

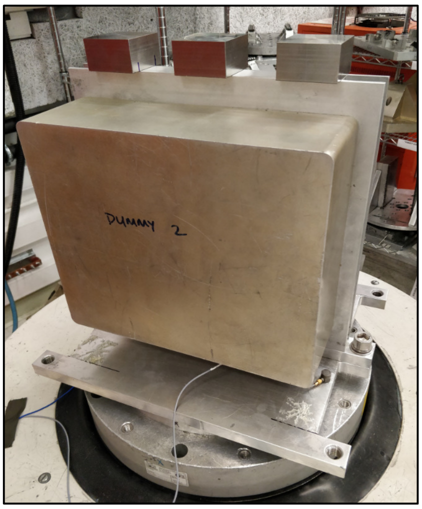

Figure 5.73. Test setup with the fourth TVA combination

Random vibration test is run again and the test is aborted as in Figure 5.74 due to high resonant behavior around 935 as somewhat is expected.

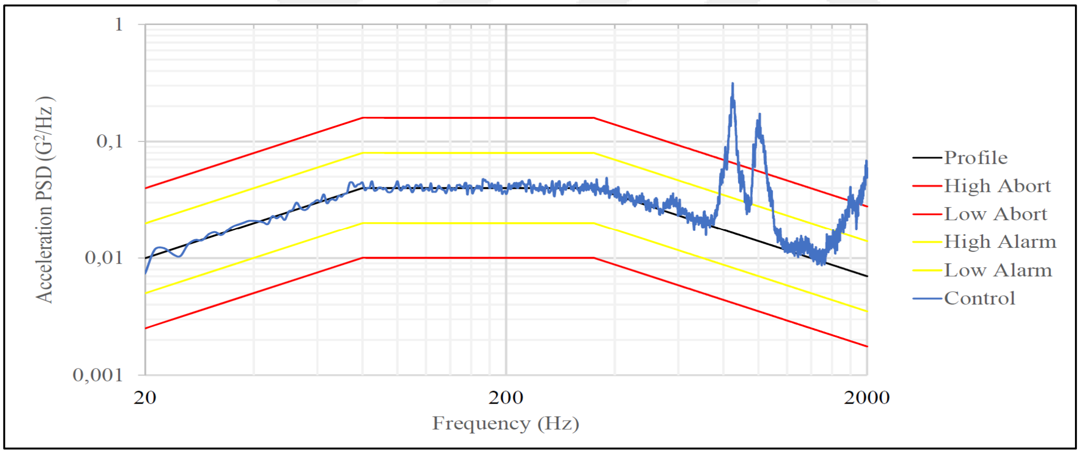

Figure 5.74. Random Vibration Test Result with the Fourth TVA Combination

5.2.6 Tabulated Data for the Applied TVA Treatments

We obtain the desired random vibration profile after two TVA treatments. Then, following two more TVA treatments are also tried and applied in order to check the performances of different TVA combinations.

After first TVA treatment, random vibration test is aborted again and the information about the first treatment combination is tabulated in Table 5.5.

Table 5.5 Information about the first TVA treatment combination

Actual Target Frequency (Random Vibration Test)	*Target Frequency (FE Model)*	*Total Effective Mass of TVAs*	**Number of 3M-467 MP layers for each TVA **Loss Factor*	*Cross section of 3M-467 MP for each TVA*	*Reduction in FE TR Plot (Initial/ Final)*	*Reduction in experimental TR Plot (Initial/ Final)*	*Random Vibration Test Status after Treatment*
935 Hz	921 Hz	(4x0.8) 3.2 kg	*17 *1.3	50x50 mm	7.66	10.45	Aborted

Due to the random vibration test fails again, it is decided to apply TVA treatment for the mode around 1780 Hz and results are tabulated as in the Table 5.6.

Table 5.6 Information about the second TVA treatment combination

Actual Target Frequency (Random Vibration Test)	*Target Frequency (FE Model)*	*Total Effective Mass of TVAs*	**Number of 3M-467 MP layers for each TVA **Loss Factor*	*Cross section of 3M-467 MP for each TVA*	*Reduction in FE TR Plot (Initial/ Final)*	*Random Vibration Test Status after Treatment*
935 Hz	921 Hz	(4x0.8) 3.2 kg	*17 **1.3	50x50 mm	5.7	Performed
1780 Hz	1759 Hz	(1x7.5) 7.5 kg	*3 **1.0	34x28 3 mm	4.20	

Desired random vibration profile is obtained after the second TVA treatment combination. Similarly, information about additional TVA treatment combinations (the third and the fourth) is tabulated as in Table 5.7 and Table 5.8 respectively.

Table 5.7 Information about the third TVA treatment combination

Actual Target Frequency (Random Vibration Test)	*Target Frequency (FE Model)*	*Total Effective Mass of TVAs*	**Number of 3M-467 MP layers for each TVA **Loss Factor*	*Cross section of 3M-467 MP for each TVA*	*Reduction in FE TR Plot (Initial/ Final)*	*Random Vibration Test Status after Treatment*
935 Hz	921 Hz	(4x0.8) 3.2 kg	*17 **1.3	50x50 mm	7.4	Out of Tolerance Bands
1780 Hz	1759 Hz	(3x1) 3 kg	*6 **1.0	34x60 mm	1.5	

Table 5.8 Information about the fourth TVA treatment combination

Actual Target Frequency (Random Vibration Test)	*Target Frequency (FE Model)*	*Total Effective Mass of TVAs*	**Number of 3M-467 MP layers for each TVA **Loss Factor*	*Cross section of 3M-467 MP for each TVA*	*Reduction in FE TR Plot (Initial/ Final)*	*Random Vibration Test Status after Treatment*
1780 Hz	1759 Hz	(3x1) 3 kg	*6 **1.0	34x60 mm	1.5	Aborted

CHAPTER 6

DISCUSSION AND CONCLUSION

In this chapter, contribution of the study is summarized and final discussion is made about the mass addition due to TVA treatments. A practical method is offered for mounting & dismounting TVAs without any damage on the viscoelastic material. Finally, conclusion is made according to all mentioned information throughout this study.

6.1 Discussion

Total mass of the vibration test fixture and two UUTs is 36.1 kg and the mass increase is 10.7 kg which is due to two TVA treatments for a successful random vibration test. It may be possible to redesign a more rigid fixture and increase total mass 10.7 kg. But it is more practical to use easily produced and reusable TVAs which saves redesign time and reproduction cost.

As we investigate the second suppressed mode around 1750 Hz, it is realized that shaker mode (1782.5 Hz) is coupled with the vibration test fixture and UUT assembly mode. Thus, it is concluded that the effective mass for this mode is equal to shaker total mass (60.9 kg) at least. By increasing the effective mass as 12%, the mode is suppressed which is a sign of an effective TVA treatment.

On the other hand, mounted TVAs should be dismounted for the other test axis configuration. 3M-467 MP is a sticky and soft material and it is damaged by the dismounting process as it is seen in Figure 6.1.

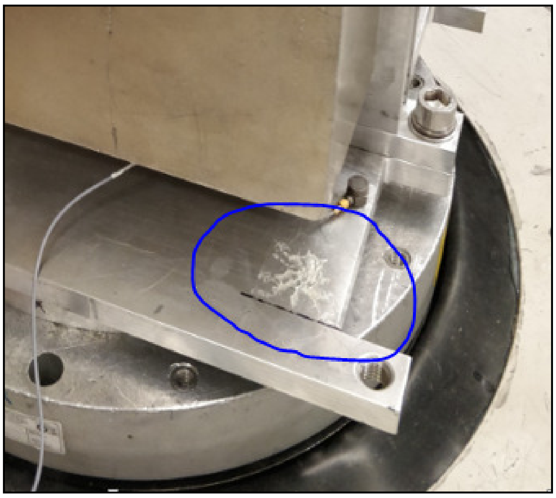

Figure 6.1. Residue of 3M-467 MP after dismounting process

Each TVA can be used with a metal adapter plate for multiple mounting & dismounting process as it is seen in Figure 6.2. Superglue or proper bolts can be used for mounting purpose and the torque is applied on the adapter plate by a wrench without any damage on the viscoelastic material.

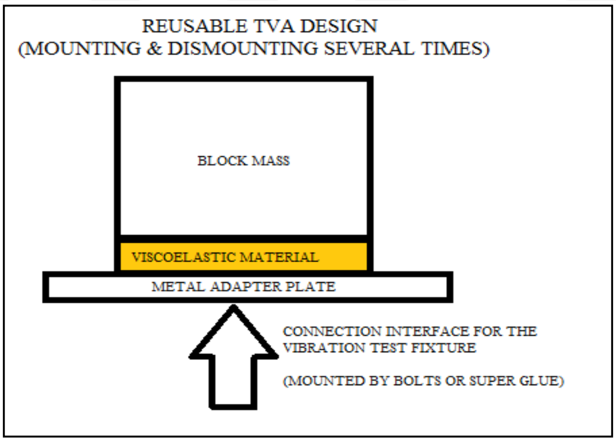

Figure 6.2. A Generic Reusable TVA Design

6.2 Conclusion

In order to design vibration test fixtures with no resonant behaviour within the test frequency range, material selection is also a crucial parameter. The material of the vibration test fixture is selected such a way that maximizes elastic modulus and minimizes density at the same time. This means that maximizing the first resonant frequency of the vibration test fixture while keeping its mass as low as possible. Mass of the vibration test fixture is also an important criteria in order not to exceed shaker load capacity to perform tests.

Specific stiffness of materials, which is the ratio of elastic modulus and density, is a good indicator of using a material to fabricate vibration test fixtures. However, commonly used metals with good machinability such as aluminum alloys and structural steels have the same specific stiffness. On the other hand, recent developments in material science technology has brought another isotropic metal alloy called AlBeMet which has a specific stiffness nearly 3.5 times greater than mentioned commercial metals. This new alloy also has good machinability characteristics based on the declaration of manufacturer but beryllium content must be taken into consideration in order to prevent health problems during machining. Besides, the major shortage of the new material is its cost and it has not been feasible to use AlBeMet as a vibration fixture material yet.

In the light of all mentioned information in this study, resonant problems of the vibration test fixture can be solved practically and economically by applying the presented damping treatment method.

Instead of applying TVA treatment to all resonant regions at the same time, it is better to start from the highest peak and treat one by one in order to take shaker controller ability into account as stated for 600 Hz region.

The developed TVA application methodology which is seen in Figure 6.3, prevents engineers to design TVAs for all problematic modes and saves time. It may be used in the vibration test industry as a guide to solve the same type of problems.

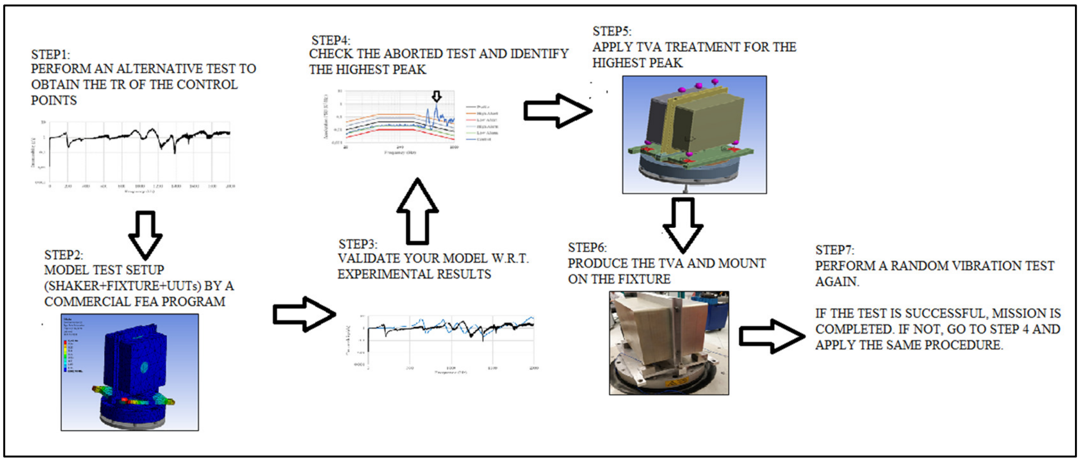

Figure 6.3. Developed Methodology

In addition, designing a TVA for high frequencies is a challenging task and it is also completed by solving the resonance problem in this study.

REFERENCES

A.D. Nashif, David I.G. Jones, J. P. H. (1985). *Vibration Damping*. Wiley.

Avitabile, P. (1999). Why you can't ignore those vibration fixture resonances. *S V Sound and Vibration*, *33*(3), 20–26.

Baker, R. (n.d.). *VibKit*. http://www.vibkit.com/book/vint_1.htm

De Barros, E., & Souto, C. D. A. (2017). Evaluation of a vibration text fixture. *International Journal of Acoustics and Vibrations*, *22*(3), 349–352. https://doi.org/10.20855/ijav.2017.22.3480

DeLima, W. J., & Ambrose, M. N. (2015). Experimental Characterization and Simulation of Vibration Environmental Test. *Conference Proceedings of the Society for Experimental Mechanics Series*, *10*, 45–55. https://doi.org/10.1007/978-3-319-15251-6

Gatscher, J. A., & Kawiecki, G. (1996). Review Comparison of Mechanical Impedance Methods for Vibration Simulation. *Shock and Vibration*, *3*(3), 223–232. https://doi.org/10.3233/SAV-1996-3308

Harvie, J. M., & Mayes, R. (2016). Quantification of dynamic differences between boundary conditions for environment specification improvement. *Conference Proceedings of the Society for Experimental Mechanics Series*, *9*, 117–132. https://doi.org/10.1007/978-3-319-30087-0_11

Jeong, H. S., & Cho, J. R. (2016). Optimal design of head expander for a lightweight and high frequency vibration shaker. *International Journal of Precision Engineering and Manufacturing*, *17*(7), 909–916. https://doi.org/10.1007/s12541-016-0111-z

Jeong, W. B., Yoo, W. S., & Kim, J. Y. (2003). Sensitivity analysis of anti-resonance frequency for vibration test control of a fixture. *KSME International Journal*, *17*(11), 1732–1738.

https://doi.org/10.1007/BF02983603

Jingze, W., Wenyuan, Z., & Pengtao, Z. (2016). Design and Mode Analysis of Random Vibration Test Fixture of Some Airborne Heat Exchangers. *IEEE/CSAA International Conference on Aircraft Utility Systems (AUS)*, *7*, 1075–1078.

Kenneth G. McConnell, P. S. V. (2008). *Vibration testing : theory and practice* (Second Edi). J. Wiley & Sons, 2008.

Kim, J. Y., Jeong, W. B., Lee, S. B., & Lee, B. H. (2001). An Experimental Approach for Structural Dynamic Modification of Fixture in Vibration Test Control. *JSME International Journal*, *44*(2), 334–340.

Kulkarni, N., & Lakkannavar, V. (2015). Optimization and Fine-tuning of a Vibration Fixture Design for Desired Dynamic Response. *Altair Technology Conference*, 1–6.

Kumar, M., Rao, T. N., Jagadisan, K., & Jayathirtha Rao, K. (2002). Tailoring of vibration test specifications for a flight vehicle. *Defence Science Journal*, *52*(1), 41–46. https://doi.org/10.14429/dsj.52.2147

LDS DACTRON. (2008). *Shaker Control User Guide*.

Li, Q.-Z., Chen, G. P., & Fang, K. (2013). Sensor placement optimization method in environmental vibration tests. *Zhendong Yu Chongji/Journal of Vibration and Shock*, *32*(8), 158–161.

Poncelet, F., Marin, F., Fleury, C., & Golinval, J. C. (2005). Optimal design of fixtures for vibration testing of structures on electro-dynamic shaker. *12th International Congress on Sound and Vibration 2005, ICSV 2005*, *6*(January 2005), 5128–5135.

Rahman, H., & Kumar, R. J. (2016). Design of a Composite Vibration Fixture for Testing Fuel Tank for Combat Vehicle Application. *International NAFEMS Conference on Engineering Analysis, Modeling, Simulation and 3D-Printing*

(NAFEMS-3D), *September*.

Rice, S. O. (1944). Mathematical Analysis of Random Noise. *Bell System Technical Journal*.

Richard G. Budynas, J. K. N. (2014). *Shigley's Mechanical Engineering Design* (Tenth Edit). Mc Graw Hill Education.

Sentek. (n.d.). *How to Select A Vibration Testing System*. https://static1.squarespace.com/static/5526e8e7e4b0356ed20c43fe/t/56904b742399a31801604a8b/1452297081937/How+to+Select+a+Vibration+Testing+System.pdf

Sisemore, C., & Harvie, J. (2017). Simultaneous qualification testing of multiple components and the influence of closely spaced vibration modes. *Conference Proceedings of the Society for Experimental Mechanics Series*, *9B*, 83–90. https://doi.org/10.1007/978-3-319-54735-0_9

Wang, K., Sun, Y., & Mao, Z. (2013). Comprehensive optimization method for dynamic design of fixture of vibration test. *Zhendong Ceshi Yu Zhenduan/Journal of Vibration, Measurement and Diagnosis*, *33*(3), 483–487.

Williams, A., Cai, V., Maestas, M., Heit, J., & Taylor, S. (2019). Multipoint Control for Single Axis Vibration Testing. *Special Topics in Structural Dynamics*, *5*, 205–213. https://doi.org/10.1007/978-3-319-75390-4_19

Yuan, H., & Li, C. (2003). Vibration environment simulation controller. *Fifth International Symposium on Instrumentation and Control Technology*, *5253*(2003), 888–892. https://doi.org/10.1117/12.522328

Zhang, J. G., & Ma, X. R. (2012). Satellite force limited sine vibration testing. *19th International Congress on Sound and Vibration*, 3049–3058.